RESEARCH ARTICLE

WILEY

Loss of *smarcad1a* accelerates tumorigenesis of malignant peripheral nerve sheath tumors in zebrafish

Han Han[1] | Guangzhen Jiang[1] | Rashmi Kumari[1] | Martin R. Silic[1] |
Jake L. Owens[2] | Chang-Deng Hu[2,3] | Suresh K. Mittal[1,3,4] | GuangJun Zhang[1,3,4,5]

[1]Department of Comparative Pathobiology, Purdue University, West Lafayette, Indiana, USA

[2]Department of Medicinal Chemistry and Molecular Pharmacology, Purdue University, West Lafayette, Indiana, USA

[3]Purdue University Center for Cancer Research, Purdue University, West Lafayette, Indiana, USA

[4]Purdue Institute for Inflammation, Immunology and Infectious Disease (PI4D), Purdue University, West Lafayette, Indiana, USA

[5]Purdue Institute for Integrative Neuroscience (PIIN), Purdue University, West Lafayette, Indiana, USA

Correspondence
GuangJun Zhang, Department of Comparative Pathobiology, Purdue University, 625 Harrison Street, West Lafayette, IN. 47906, USA.
Email: gjzhang@purdue.edu

Present address
Guangzhen Jiang, College of Animal Science and Technology, Nanjing Agricultural University, Nanjing, China

Abstract

Malignant peripheral nerve sheath tumors (MPNSTs) are a type of sarcoma that generally originates from Schwann cells. The prognosis for this type of malignancy is relatively poor due to complicated genetic alterations and the lack of specific targeted therapy. Chromosome fragment 4q22-23 is frequently deleted in MPNSTs and other human tumors, suggesting tumor suppressor genes may reside in this region. Here, we provide evidence that *SMARCAD1*, a known chromatin remodeler, is a novel tumor suppressor gene located in 4q22-23. We identified two human homologous *smarcad1* genes (*smarcad1a* and *smarcad1b*) in zebrafish, and both genes share overlapping expression patterns during embryonic development. We demonstrated that two *smarcad1a* loss-of-function mutants, sa1299 and p403, can accelerate MPNST tumorigenesis in the *tp53* mutant background, suggesting *smarcad1a* is a *bona fide* tumor suppressor gene for MPNSTs. Moreover, we found that DNA double-strand break (DSB) repair might be compromised in both mutants compared to wildtype zebrafish, as indicated by pH2AX, a DNA DSB marker. In addition, both *SMARCAD1* gene knockdown and overexpression in human cells were able to inhibit tumor growth and displayed similar DSB repair responses, suggesting proper *SMARCAD1* gene expression level or gene dosage is critical for cell growth. Given that mutations of *SMARCAD1* sensitize cells to poly ADP ribose polymerase inhibitors in yeast and the human U2OS osteosarcoma cell line, the identification of *SMARCAD1* as a novel tumor suppressor gene might contribute to the development of new cancer therapies for MPNSTs.

KEYWORDS
CRISPR, MPNST, *SMARCAD1*, *smarcad1a*, *tp53*, DNA damage repair, zebrafish, 4q22-23

1 | INTRODUCTION

Cancer is essentially a genetic or genomic disease, as there are many genetic alterations in cancer cell genomes.[1] Based on their functions,

genes can be classified as either cancer driver genes or passenger genes. The cancer driver genes (*i.e.*, oncogenes and tumor suppressor genes) are the genes whose mutations directly contribute to cancer initiation, development, and metastasis. In contrast, the genes whose mutations are not directly related to cancer are passenger genes.[2] It is challenging to identify cancer driver genes even with high throughput

Han Han, Guangzhen Jiang, and Rashmi Kumari equally contributed to this article.

microarray and genome sequencing technologies.[3] One of the most challenging types of genetic alterations is arm-level copy number alterations (CNAs), which are synonymous with aneuploidy in terms of cytogenetics.[4] There are usually hundreds of genes on such an arm-level CNA, and the gene dosage of each of these genes is affected by the large CNA. Unless the cancer driver genes also exhibit point mutations, there is almost no way to sort the driver genes apart from the passenger genes. Cross-species comparative oncogenomics serves as one powerful solution for identifying cancer drivers on large CNAs due to genes conservative functions.[5-8]

Malignant peripheral nerve sheath tumors (MPNSTs) are a rare type of sarcoma (∼2% of all sarcomas) originating from the neural crest or Schwann cell lineage with an incidence rate of five per million each year.[9] The prognosis for MPNSTs is generally poor due to their complex genetic changes within tumors, invasive growth nature, and insensitivity to chemo- and radiotherapies.[10-12] Targeted cancer therapy is one of the mainstays of the current cancer treatment regime because of its high specificity and reduced side effects. Unfortunately, there is no targeted therapy currently available for this type of malignancy. This is mainly caused by the lack of knowledge about the cancer driver genes of MPNSTs. Chromosome fragment 4q22-23 is frequently deleted in MPNSTs and many other types of human cancers.[13-21] However, the critical cancer driver genes on this CNA remain largely unknown.

Zebrafish have become a popular organism for modeling human cancer due to their large number of offspring, tractable genetics, and amenability to in vivo imaging as well as chemical screening.[22] Numerous zebrafish genetic models confirm that, between humans and zebrafish, there is functional conservation of known core cancer genes, such as tp53, pten, Myc, mutant KRAS, and mutant BRAF.[23-27] Since human and zebrafish genomes share small syntenies, due to extensive reshuffling of genes' locations during evolution, we have demonstrated that zebrafish–human comparative cancer genomics is an effective approach for pinpointing cancer driver candidates on large CNAs in MPNSTs.[8] Utilizing the zebrafish–human comparative cancer genomics approach, we narrowed a limited number of tumor suppressor candidate genes in chromosome fragment 4q22-23.[8] One of them is SMARCAD1 (SWI/SNF-related, matrix-associated actin-dependent regulator of chromatin, subfamily a, containing DEAD/H box 1). SWI/SNF and other chromatin remodelers are frequently reported as cancer driver genes in many types of human cancers.[28-30] A recent study revealed that one of the SWI/SNF family members, SMARCA2, is commonly mutated in human MPNSTs.[31] Thus, we decided to focus on the SMARCAD1 gene in the current study.

SMARCAD1 is a chromatin remodeler that belongs to the SNF2 helicase subfamily, which possesses a conserved ATP-helicase domain.[32] Human SMARCAD1 was also reported to cooperate with the E1A oncogene to increase gene reactivation events by genomic rearrangement, suggesting its roles in maintaining genomic stability.[21] The homologous yeast gene, Fun30/Fft3, was found to play an essential role in the end resection of DNA double-strand break (DSB) repair and heterochromatin maintenance.[33-35] In human cells, SMARCAD1 is preferentially involved in homologous recombination after DNA DSB (double strand break) repair during S-phase, and this process depends on ATM (ataxia-telangiectasia).[36]

In addition, defects in FUN30 were reported to be sensitive to DNA topoisomerase 1 (TOP1) and poly ADP ribose polymerase (PARP) inhibitors in yeast and the U2OS cancer cell line.[33,37] Moreover, SMARCAD1 was recently found involved in mismatch repair,[38] and endogenous retroviral silencing,[39] both critical for genomic stability. A more recent study also backed up its critical roles in maintaining genomic integrity by stabilizing the replication forks.[40] In humans, SMARCAD1 gene mutations were found associated with skin cancer susceptibility, adermatoglyphia, and Basan syndrome.[41-43] However, the in vivo tumorigenic roles of the SMARCAD1 gene in MPNSTs remain unexplored.

Here, we provide evidence for the first time that zebrafish smarcad1a functions as a tumor suppressor gene in vivo. Moreover, we demonstrate that the human SMARCAD1 gene dosage is essential for MPNST cells to maintain genomic stability in response to DNA damage. Since it is known that the SMARCAD1 mutation causes yeast and U2OS osteosarcoma cell lines to become sensitive to PARP inhibitors, identifying SMARCAD1 as a tumor suppressor gene may provide us a new potential therapeutic target for some MPNST patients with currently available PARP inhibitors.

2 | MATERIALS AND METHODS

2.1 | Zebrafish lines, husbandry, and tumor onset analysis

Zebrafish were raised and maintained at the Purdue animal housing facility, which is approved by AAALAC. All experiments were carried out according to the protocols approved by the Purdue Animal Care and Use Committee (PACUC). The sa1299 fish were purchased from ZIRC (zebrafish international resource center). All the fish husbandry was carried out according to the zebrafish book.[44] The tumor-prone zebrafish line carrying the $tp53^{M214K/M214K}$ point mutation has been described previously.[8,25] After crossing, PCR genotyping was carried out at 6–8 weeks of age using previously published genotyping methods for $tp53$.[8,25] Siblings of different genotypes were housed in adjacent tanks at similar densities to minimize environmental differences. During tumorigenesis monitoring, fish were euthanized at first observation of tumors or other signs of illness. The tumor types of the euthanized fish were confirmed by examining the hematoxylin and eosin (HE) stained tumor sections by a board-certified veterinary pathologist blinded to the experimental groups.

2.2 | Sa1299 mutant fish genotyping and mRNA splicing analysis

For sa1299 fish, gDNA was prepared from caudal fin clips with the hotshot protocol[45] with the following modifications: boiling in 100 μl NaOH (50 mM) at 95°C for 1 h, then neutralized with 10 μl 1 M Tris-HCl pH 8.0 per sample. PCRs were performed using primers designed to distinguish between the mutant and wild-type sequences. For wild-type alleles, primers sa1299-F and sa1299-WR were used, and the sa1299-F and sa1299-WR were used to detect mutant alleles. For both PCRs, mIEXON5.WT.FW and UMLEXON5.RV were included as

internal controls. Both PCRs resulted in a 391 bp product for the *smarcad1a* allele and a 239 bp product for the internal control primers. Conditions for both PCRs were 95°C 2 min, (95°C 30 s, 65.5°C 30 s, and 72°C 60 s) × 35 cycles, 72°C 10 min, and 10°C 2 min. PCR products were analyzed on 2% agarose gels with ethidium bromide staining and imaged using GelDoc-IT2 imaging system (UVP).

To analyze mRNA splicing, total RNAs were isolated from 1dpf homozygous and wildtype fish embryos using Trizol reagent. The RNAs were treated with DNAase I to remove possible gDNA contamination. The reverse transcriptions were performed with SuperScript III Reverse Transcriptase (Thermo Scientific) and Oligo(dT)$_{18}$ following manufactory protocol. Full length and partial cDNA (exon8-exon10) were amplified with GXL Taq (Takara) using the cDNA as a template and primers listed in Table S1. The PCR products were then cloned into the pJET1.2 vector using the blunt ligation kit. Sanger sequencing was performed using the primer smarcad1a-exon8-F.

2.3 | *Smarcad1a* CRISPR mutant generation

CRISPR gRNAs, *smarcad1a*-CR383 (5′ GCGGATGGTCAGTTTCCATC 3′) and *smarcad1a*-CR490 (5′ GCAGCATATAAACAAGGACA 3′), were designed against the exon3 and exon4 of ENSDART00000091409, respectively (Figure 6). Oligonucleotides were synthesized by IDT (Integrated DNA Technologies Inc.) and were cloned into DR274 vector following the published method.[46] Briefly, both sense and antisense oligonucleotides were annealed to dsDNA, double-stranded DNA (95°C 10 min, and then ramp down to 12°C at 5°C/min). DR274 plasmid was digested with BsaI (NEB) to generate compatible ends with the annealed oligonucleotides, and the dsRNAs were inserted into the DR274 with T4 DNA ligase (NEB). CRISPR clones were finally verified by Sanger Sequencing. To generate the gRNAs for injections, the DR274 vector was first linearized with DraI (NEB) and used as the template for the transcription reaction with T7 RNA polymerase (NEB). All the gRNAs were purified by RNA Clean & Concentrator kit (Zymo, #R1017). All injections were performed at the one-cell stage of zebrafish embryo development.[47] For each embryo 2 nl of the following mixture was injected; 12.5 ng/μl gRNA, 100 ng/μl Cas9 protein (NEB), and 0.4% phenol red (Sigma, P0290). The injected adult F_0 fish were outcrossed with wild-type fish, and around 20 fish embryos from each pair were sacrificed for gDNA isolation. PCR assays were performed to screen out positive F_0 fish. Briefly, pooled fish embryos were put into 100 μl of DNA lysis buffer (50 mM NaOH) and heated at 95°C for 60 min, then allowed to cool to room temperate and 10 μl Tris-HCl pH 7.9 was added to neutralized the lysis buffer.[45] Then, PCRs were performed using the gDNA and smarcad1a-F3 and smarcad1a-R3 primers (Table S1). The wildtype allele yields a 539 bp PCR product, while a 296 bp PCR product is generated in the *smarcad1a*^{p403} mutant. Once a positive F_0 was identified, the rest of fish embryos from the same cross were raised to adulthood as F_1 founder fish. To clean out possible off-target mutants, we continually out-crossed the F1 founders with wildtype fish twice for F_2 and F_3. Then, F_3 were in-crossed for generating homozygous F_4 smarcad1a mutants. All the experiments were performed on fish embryos from the F_4 fish cross.

2.4 | Quantitative RT-PCR

Total RNAs were isolated from cells using TRIzol reagent according to the manufacturer's instruction. For reverse transcription, 2 μg total RNA was used as a template, and cDNAs were synthesized using the Transcriptor First Strand cDNA Synthesis Kit (Roche). QRT-PCRs were conducted using SYBR Green I Master Mix (Roche), following the manufacturer's instruction on Light Cycler 480. Primers (Table S1) for each gene were designed to cover all the transcripts, which are located on different exons to avoid potential genomic DNA contamination. PCRs were performed at the following condition: 95°C, 10 s; 60°C, 15 s; and 72°C, 20 s for 40 cycles. Results were analyzed using ΔCt method to calculate the relative gene mRNA level.[48]

2.5 | SMARCAD1 phylogeny, synteny, and gene structure analyses

SMARCAD1 protein sequences were identified by a BLASTp search using the human SMARCAD1 sequence as a query in Ensembl and NCBI. The longest sequence was preferentially chosen when there were multiple sequences. Multiple protein sequences (Table S2) were aligned using the MUSCLE alignment program.[49] The evolutionary model for phylogenetic analysis was identified using the best model test using maximum likelihood and default parameters in MEGA6.[50] A minimum evolution phylogeny was generated in MEGA6 with complete deletion option: bootstrap = 10 000; gamma = 0.61. A maximum-likelihood phylogenetic tree was constructed using JTT + G with 1000 bootstrap replicates with PhyML 3.1.[51] For Bayesian analysis (BP) phylogenetic analysis, 20 million generations were run using the following parameters in MrBayes 3.2.6: nruns = 2, nchains = 4, aamodel = fixed (Jones), rates = gamma ngammacat = 8, samplefreq = 500, burninfrac = 0.25. The final phylogenetic trees were viewed and generated with FigTree V1.4.2 (http://tree.bio.ed.ac.uk/software/figtree). Gene intron-exon structures were analyzed using the longest transcripts in Ensembl.

Synteny analyses were performed with the teleost synteny database[52] and verified with Ensembl and UCSC human and zebrafish genome databases. The *SMARCAD1* exon-intron structure analysis was performed in the UCSC genome browser, and the Gene structure display server was used for visualization using the information of the *smarcad1a* gene downloaded from the table genome annotation in the UCSC zebrafish genome (GRCz11). SMARCAD1a protein domains were predicted by online SMART analysis using the default settings.[53]

2.6 | Gene cloning, whole-mount in situ hybridization, and imaging

Full-length coding regions of zebrafish *smarcad1* genes were amplified by RT-PCR using gene-specific primers designed according to the current DNA sequence in Ensembl. Phusion® High-Fidelity DNA Polymerase master mix (New England Biolabs) was used for PCR

amplification. PCR primers used here are listed in Table S1. The PCR products were purified using Zymo Gel Extraction Kit (Zymo Research) before they were cloned into the pJet1.2 vector using the CloneJET PCR Cloning Kit (Thermo Scientific). Gene inserts orientation was verified by Sanger sequencing. Riboprobes were synthesized through in vitro transcription using T7 DNA polymerase (New England Biolabs) and DIG RNA Labeling Mix (Roche). Then, the riboprobes were purified by SigmaSpin™ post-reaction clean-up columns (Sigma, S5059). Whole-mount in situ hybridization was carried out according to our previously published method.[54,55] For histological analysis, post-hybridization embryos were equilibrated in 15% sucrose, then 30% sucrose in 20% gelatin, after which they were embedded in 20% gelatin for cryosectioning (6–12 μm). Images were acquired using AxioCam MRc camera on Zeiss SteREO Discovery.V12 and Axio Imager 2 compound microscope.

2.7 | Cell culture, stable cell lines, and cell growth assays

All experimental protocols using cell lines and plasmid constructs were approved by the Purdue University institutional biosafety review board. The human MPNST cell lines were authenticated by ATCC using short tandem repeat profiling. Cells were cultured in DMEM with 10% heat-inactivated fetal bovine serum, penicillin (100 IU/ml), and streptomycin (100 μg/ml). All cell cultures were carried out at 37°C in a humidified 5% CO_2 atmosphere. A full-length sequence of the SMARCAD1 gene was amplified from HEK293T cells and was confirmed by Sanger sequencing. The SMARCAD1 gene was subsequently cloned into pLIX408, a T2A bicistronic lentiviral vector modified from pLIX402 (Addgene #41394). For SMARCAD1 gene knockdown, shRNAs against human SMARCAD1 gene and non-targeting shRNA control were purchased from TransOMIC technologies Inc. (ULTRA-3351709, ULTRA-3351712, ULTRA-3351713). Stable cell establishment, western blots, MTT, and plate agar assays were conducted as described previously.[56] For Western blot, a commercial anti-SMARCAD1 antibody (Bethyl, A301-593A 1:2000 dilution) was chosen. Statistical analyses were performed using GraphPad Prism 6.0h. Data were analyzed using the unpaired student t test. $p < 0.05$ was considered to have a statistically significant difference.

2.8 | Immunohistochemistry

Zebrafish with tumors were fixed with 10% neutral buffered formalin (VWR). Dehydration, paraffin section, and H&E staining were performed in the Histology Research Laboratory, College of Veterinary Medicine, Purdue University. Slides with adjacent sections were dewaxed with xylene (2 × 10 min) to remove paraffin and followed by rehydration with a series of diluted ethanol (100%, 95%, 80%, 50%, 5 min each) and water rinse. Next, heat-mediated antigen retrieval was performed to unmask the antigenic sites: all the sections were incubated at 95°C for 10 min in Tris/EDTA buffer (pH 9.0). Then, 3%

hydrogen peroxide was used to block endogenous peroxidase in tissue for 10 min, followed by 5 min tap-water rinsing and 2.5% goat serum blocking for 2 h. The primary antibody (anti-S100: Dako #IS504; anti-H3K27me3: Millipore #07-499, 1:500 dilution in 2.5% goat serum) was incubated with sections in a 4°C humidity chamber overnight. On the second day, sections were washed with Tris-buffered saline (TBS) 3 times. Then the primary antibody was visualized with the avidin/biotin-based peroxidase system (VECTASTAIN Elite ABC-HRP kit, #PK-6101; DAB Substrate Kit, #SK-4100, Vector Laboratories, CA, USA) by following the manufacturer's instructions. Briefly, sections were incubated with biotinylated goat anti-rabbit antibody for 30 min, followed by three times TBS wash. Then all the sections were incubated with ABC reagent for 30 min. After three times wash with TBS, 3,3′-diaminobenzidine (DAB) substrate was used to label primary antibody binding tissues. Next, sections were counterstained with hematoxylin and dehydrated with gradient dilutions of ethanol (80%, 95%, 100%, and 100%). Sections were then cleared by xylene and mounted with Cytoseal 60 mounting medium (Epredia™ 83 104). Images of stained sections were taken with Zeiss Axio imager A2.

2.9 | DNA damage repair response

Human cells with stable SMARCAD1 overexpression and knockdown (both doxycycline induced and un-induced) were treated with X-ray irradiation treatment. They were then harvested and lysed using RIPA buffer with 0.5 mM PMSF (phenylmethylsulfonyl fluoride). The indicated doses of radiation were administered using the X-RAD 320 biological irradiator device (PXi Precision X-Ray, North Branford, CT, USA). Radiation was produced via an X-ray tube radiation source with a dose rate of ∼1 Gy/ 25 s. Samples were irradiated in Petri dishes at room temperature (∼25°C), and non-irradiated samples were mock irradiated.

Zebrafish embryos were collected and raised in 10 cm diameter Petri dishes with system water (0.6 g/L aquarium salt in RO water) and 0.01 mg/L methylene blue until they reached 1 day old. Chorions were removed with pronase (1 mg/mL) in the fish system water and rinsed at least 3 times with calcium-free Ringer's solution (116 mM NaCl; 2.9 mM KCl; 5 mM HEPES, pH 7.2). Then, the fish embryos were transferred into 1.5 ml Eppendorf tubes to remove the yolks from fish embryos, according to the zebrafish book.[44] Briefly, after adding 1 ml deyolking buffer (calcium-free Ringer's solution with 0.3 mM PMSF and 10 mM EDTA), yolks were separated by triturating the fish embryos with 1000 ml pipette tips. Then, the Eppendorf tubes were centrifuged at 200 rpm for 30 s, and the supernatant with yolk components was removed. Lastly, fish embryos were rinsed three times with ice-cold calcium-free Ringer's solution before adding RIPA Lysis Buffer with a complete EDTA-free protease inhibitor cocktail (5892791001) and PhosSTOP phosphatase inhibitor (4906837001). Total protein concentration was measured using the Bradford method. Approximately 30 μg total protein was run on a 15% SDS-PAGE. Anti-phospho-histone H2A. X (Ser139) (Millipore #05-636, 1:2000 dilution) was used for detecting broken double-strand DNAs using western blot. Beta-actin (ACTB,

Santa Cruz, sc-47 778, 1:2000 dilution) was used to ensure equal protein loading. Band/protein intensity was quantified using Image Lab™ (Bio-rad, Hercules, CA, USA).

2.10 | Data availability

Reagents are available upon request. The authors affirm that all data necessary for confirming the conclusions of the article are present within the article, figures, and tables.

3 | RESULTS

3.1 | SMARCAD1 is a tumor suppressor candidate on the chromosome fragment 4q22-23

Deletions of 4q22-23 are frequent in MPNSTs and many other types of human cancers, suggesting tumor suppressor genes may be located in this region. SMARCAD1 is one of the potential tumor suppressor gene candidates (Figure 1A–C). Given the importance of chromatin remodelers in cancer biology, especially the recent report on the frequent loss of SMARCA2 in MPNSTs,[31] we further examined SMARCAD1 gene mutations in TCGA data through cBioportal.[57] We found it is frequently mutated in various human cancers (uterine, skin, colorectal, sarcoma, etc.), although human MPNST data are not currently available (Figure 1D,E). We reasoned that SMRACAD1 expression might be lower if it is a tumor suppressor gene in human MPNSTs. To test this, we examined six human MPNST cell lines and found SMARCAD1 protein levels are indeed relatively lower (three significantly, and three mildly) compared to a schwannoma cell line, HEI-193 (Figure 1F). Altogether, these results suggest the SMARCAD1 could be a tumor suppressor gene.

3.2 | Zebrafish have two smarcad1 orthologues

To examine the tumor suppressor function of the smarcad1, we decided to take advantage of the zebrafish MPNST model. In zebrafish, there are two smarcad1 genes on different chromosomes:
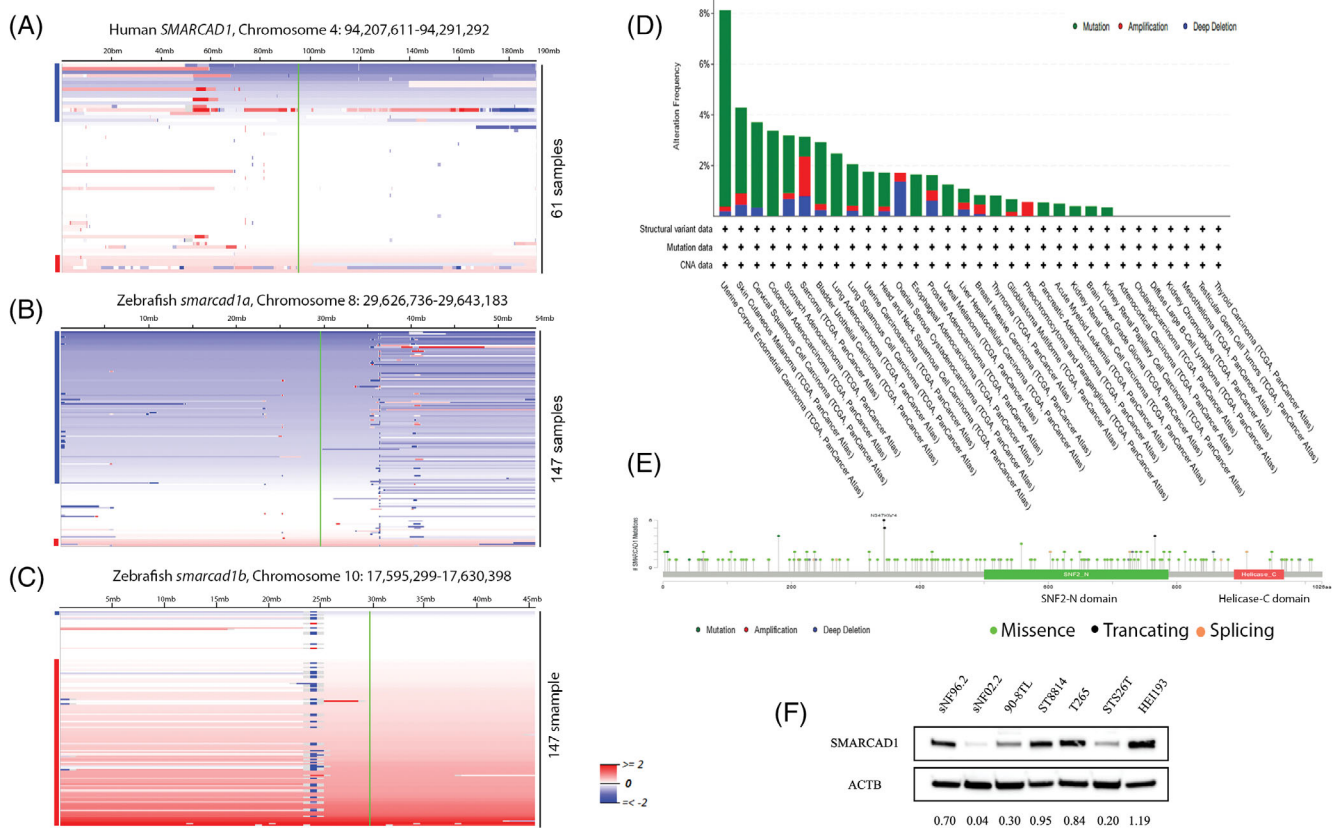

FIGURE 1 Frequent mutations of SMARCAD1 in humans and zebrafish suggest it is a tumor suppressor. (A) Heat map of human chromosome 4. SAMRCAD1 is located on this chromosome. The locus of SMARCAD1 (green line) was found to be underrepresented in ~26% (16 out of 61) human MPNSTs.[8] (B) Zebrafish smarcad1a is located on chromosome 8, which is underrepresented in about 70% (103 out of 147) of zebrafish MPNSTs. (C) Zebrafish smarcad1b is located on chromosome 10, which is overrepresented in about 60% (88 out of 147) of zebrafish MPNSTs. Samples are sorted top-to-bottom by decreasing deletion amplitude at the respective SAMRCAD1/smarcad1 locus, indicated by a green line. Blue and red bars on the right side of each panel indicate samples with SAMRCAD1/smarcad1 losses (blue) or gains (red). Color densities are corresponding to the degree of loss and gain as previously described.[8] (D) SMARCAD1 mutation frequency of human cancers in TCGA database. (E) SMARCAD1 mutation types and positions found in human cancers in TCGA database. (F) SMARCAD1 expression level of 6 human MPNST cell lines (all NF1 mutant except STS26T) and HEI-193, immortalized human schwannoma

smarcad1a and smarcad1b. To reveal the genetic relationships between zebrafish smarcad1 and other vertebrate SMARCAD1 genes, we first performed multiple phylogenetic analyses by Bayesian analysis [BP], maximum likelihood [ML], and minimum evolution [ME] method, respectively). Our results consistently support that smarcad1a and smarca1b are orthologous to the human SMARCAD1
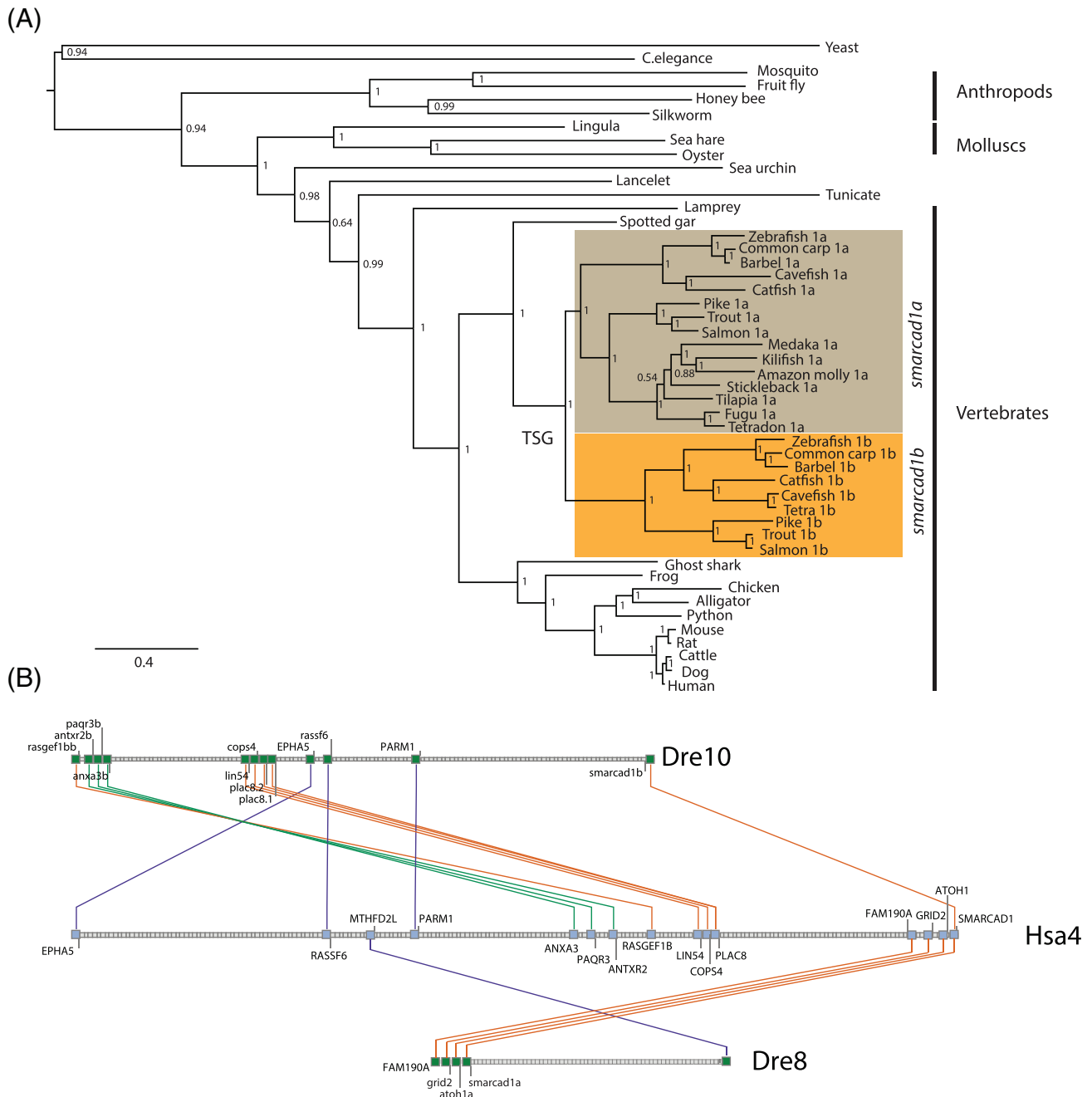

FIGURE 2 Zebrafish have two smarcad1 genes. (A) Extended majority-rule consensus tree for the Bayesian phylogenetic analysis of SMARCAD1 proteins. Numbers at each node indicate posterior probability (pp) values based on 20 million runs. Branch lengths are proportional to the means of the pp densities for their expected replacements per site. The ME and ML phylogenetic trees (Figures S1 and S2) were generally in agreement with the BP phylogeny: most of the metazoan species have one SMARCAD1 gene, while there are usually two smarcad1 genes in teleost genomes. The two smarcad1s most likely resulted from teleost-specific whole-genome duplications, as each formed a distinct clade. The tree was rooted with yeast. (B) Syntenic relationship between human and zebrafish chromosomes. Zebrafish chromosome 8 (Dre8) that contains smarcad1a and three other genes (FAM190A, GRID2, and ATOH1, bottom row) are orthologous to, and in the same order as, genes in the portion of human chromosome 4 (Hsa4) that contains SMARCAD1 (middle row). A portion of Dre10 contains smarcad1b, but not the other three directly linked genes. However, this part of Dre10 is co-orthologous to the portion of Hsa4 that contains SMARCAD1, as they share other syntenies (top row). Orthologous genes are indicated with colored lines

gene (Figure 2A; Figures S1 and S2). Since most teleosts have two smarcad1 genes, our results suggest that the two genes resulted from teleost-specific whole-genome duplication.[58-60] To further validate whether the two genes are orthologous to the human *SMARCAD1* gene, we performed syntenic analysis using the established zebrafish–human synteny database.[52] The *smarcad1a* gene is located
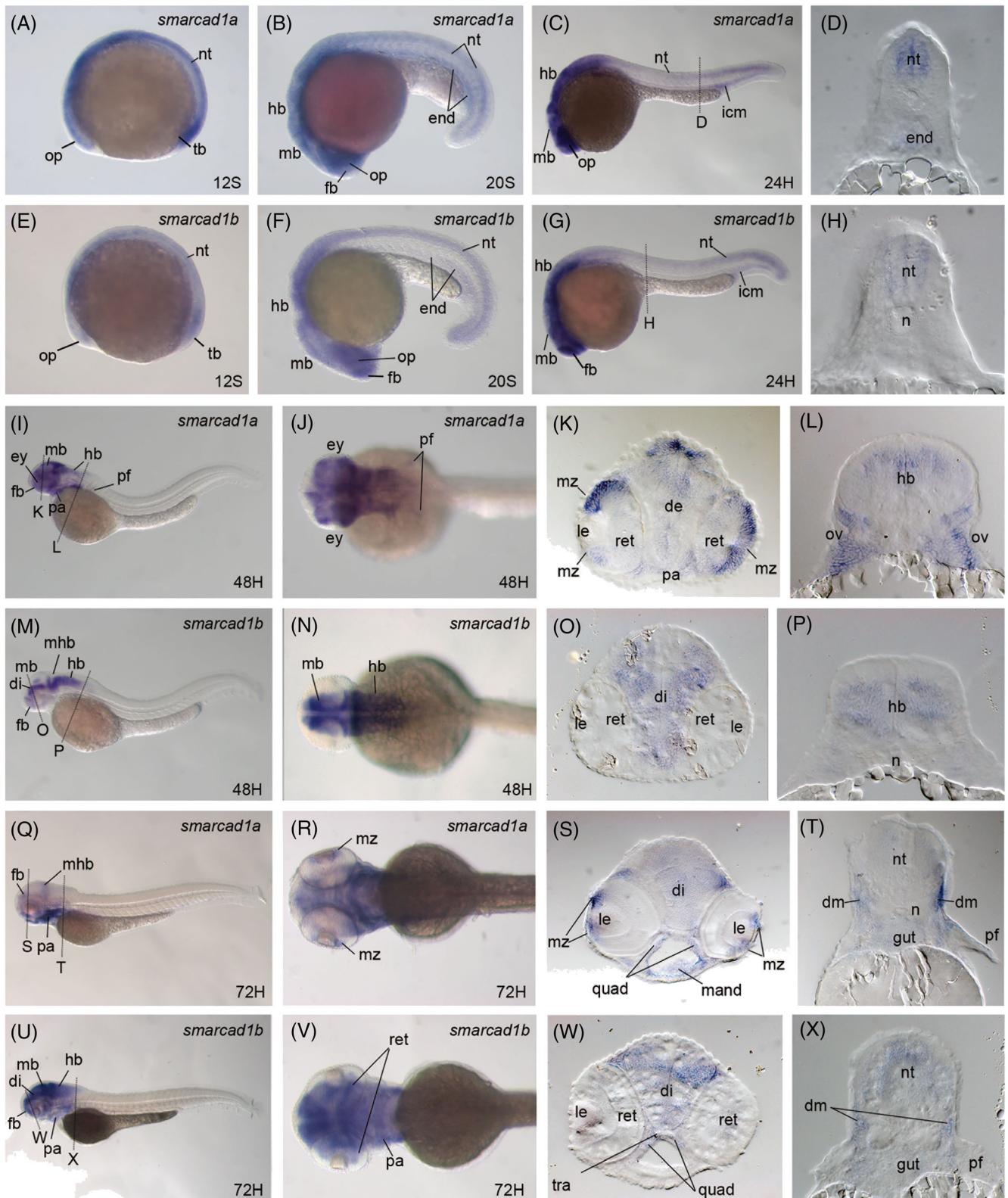

FIGURE 3 Legend on next page.

on zebrafish chromosome 8, and it shares a conserved synteny with the human SMARCAD1 gene, which is located on human chromosome 4 (Figure 2B). Zebrafish smarcd1b is located on chromosome 10, and no neighbor genes of the conserved synteny are found around the gene locus (Figure 2B). However, the nearby regions of zebrafish chromosome 10 share conserved syntenies (LIN54-PLAC8 and ANX3-RASGEF1B) with human chromosome 4 (Figure 2B), suggesting that the smarcad1b-linked neighbor genes were lost during evolution.

3.3 | The zebrafish smarcad1 genes share overlapping and distinct expression patterns during early development

Paralogous genes, resulting from whole-genome duplication, may have undergone neofunctionalization (new functions), or sub-functionalization (split functions of their parental gene) according to the duplication-degeneration-complementation (DDC) model.[61] To explore the functional relationship of two zebrafish smarcad1 genes, we examined gene expression patterns using whole-mount in situ hybridization in the zebrafish's early developmental stages. We found that both genes are expressed at the 12S (12-somite) stage in the brain, optical vesicle, neural tube, and tailbud (Figure 3A,E). The expression extended to the endoderm at the 20-somite stage (Figure 3B,F). At 24 hpf (hours post-fertilization), both genes are expressed mainly in the head region, neural tube, and intermediate cell mass (Figure 3C,D,G,H). The differential expression patterns of the two genes become evident at 48hpf (Figure 3I–P). The smarcad1a gene is mainly expressed in the eye (retina and ciliary marginal zone), brain, and pharyngeal arches (Figure 3I–L), while the smarcad1b gene is primarily expressed in the brain (Figure 3M–P). At 72hpf, smarcad1a expression in the brain region is decreased, but its expression in the ciliary marginal zone of the eye and pharyngeal arches remains (Figure 3Q,R). Cross-sections revealed that smarcad1a is also expressed in the gut and dermomyotome around the pectoral fin (Figure 3S,T). In contrast to smarcad1a, smarcad1b is mainly expressed in the brain but also found in the retina, gut, and dermomyotome

(Figure 3U–X). The overlapping and different spatiotemporal expression of the two zebrafish smarcad1 genes suggests that there was a sub-functionalization after the teleost whole-genome duplication. Moreover, these similar expression patterns indicate that the two genes may possess overlapping functions during zebrafish development and normal physiology.

3.4 | Sa1299 is a smarcad1a loss-of-function mutant

To investigate the tumor suppressor roles of the smarcad1a gene, we acquired a currently available splicing site mutant, sa1299, which was generated with ENU (N-ethyl-N-nitrosourea) by the Zebrafish Mutation Project (ZMP).[62] We first confirmed that there is a T to G mutation at the essential spicing site of intron 9 by PCR and Sanger sequencing (Figure 4A). Based on bioinformatics analysis, this mutation only changes one amino acid in the short transcript (ENSDART00000139029) but may lead to open reading frameshifting or premature truncation for the longer transcript (ENSDART00000091409). Since the essential splice site mutation may lead to intron retaining, exon skipping, or cryptic splicing, we sequenced the region between exon 7 and exon 10 of the mature mRNA from sa1299 homozygous 1dpf (day post-fertilization) zebrafish embryos. When compared to the wildtype smarcad1a mRNA, we found that the mutant mRNA is spliced through a proximal cryptic splicing site 11 bps downstream of the mutant site, and this led to the insertion of 13 bps (GGAAGGATCTGCT) in intron 9 between exon 9 and exon 10 (Figure 4B and Figure S3). This insertion resulted in a premature stop codon and a truncated protein of about 379 amino acids (Figure 4C). In zebrafish, mutant genes with point mutations are usually found down-regulated through nonsense-mediated mRNA decay.[63,64] We then tested this possibility by examining the smarcad1a gene expression levels in 1dpf sa1299 homozygous fish embryos with quantitative RT-PCR (Figure 4D). Indeed, the overall expression was reduced by more than 50% compared to wild-type zebrafish embryos. Furthermore, the decrease of smarcad1a gene expression levels was confirmed by

FIGURE 3 The two smarcad1 zebrafish genes are expressed in both overlapped and distinct regions during embryonic development. Whole-mount in situ hybridization of zebrafish embryos at stages 12S (A, E), 20S (B, F), 24 hpf (C, D, G, H), 48 hpf (I–P), and 72 hpf (Q–X). Anterior is to the left in all whole-mount images, and dorsal is to the top in all transverse sections. Gene names are labeled at the upright corner in the panels of whole-mount images. (A–D, I–L, and Q–T): gene expression of smarcad1a. (E–H, M–P, and U–X): gene expression of smarcad1b. (A and C) Lateral view of the expression of smarcad1a at 12S, 20S, and 24dpf, respectively. (D) Transverse section through the trunk region of the embryos in panel C. smarcad1a is mainly expressed in the neural tissues, endoderm, and intermediate cell mass at these stages. (E and G) Lateral view of the expression of smarcad1b at 12S, 20S, and 24dpf, respectively. (H) Transverse section through the trunk region of the embryos in panel G. The expression patterns of smarcad1b are very similar to smarcad1a at these early stages. (I, J) Lateral and dorsal view of the expression of smarcad1a at 48 hpf. (K and L) Transverse section through the head and pectoral fin regions. (M and N) Lateral and dorsal view of the expression of smarcad1b at 48 hpf. (O and P) Transverse section through the head and pectoral fin regions. (Q and R) Lateral and dorsal view of the expression of smarcad1a at 72 hpf. (S and T) Transverse section through the head and pectoral fin regions. (U and V) Lateral and dorsal view of the expression of smarcad1b at 72 hpf. (W and X) Transverse section through the head and pectoral fin regions. The dashed lines indicate the positions of sections. The letters below the dashed lines correspond to the panels. de, diencephalon; dm, dermomyotome; end, endoderm; fb, forebrain; hb, hindbrain; icm, intermediate cell mass; ir, iris; le, lens; mand, mandibular cartilage; mb, middle brain; mhb, midbrain-hindbrain boundary; mz, ciliary marginal zone; n, notochord; nt, neural tube; op, optical cup; pf, pectoral fin; pa, pharyngeal; quad, quadrate cartilage; ret, retina; tb, tail bud

whole-mount *in situ* hybridization in 1–3 dpf fish embryos (Figure 4E). Thus, sa1299 is a *smarcad1a* loss-of-function mutant. The *smarcad1a* gene is dispensable since both heterozygous and homozygous sa1299 fish can survive to adulthood without any

evident sickness or morphological abnormalities. This might be due to the functional overlap with the *smarcad1b* gene since both share close expression domains during zebrafish early development. To test this, we examined the *smarcad1b* gene expression in sa1299
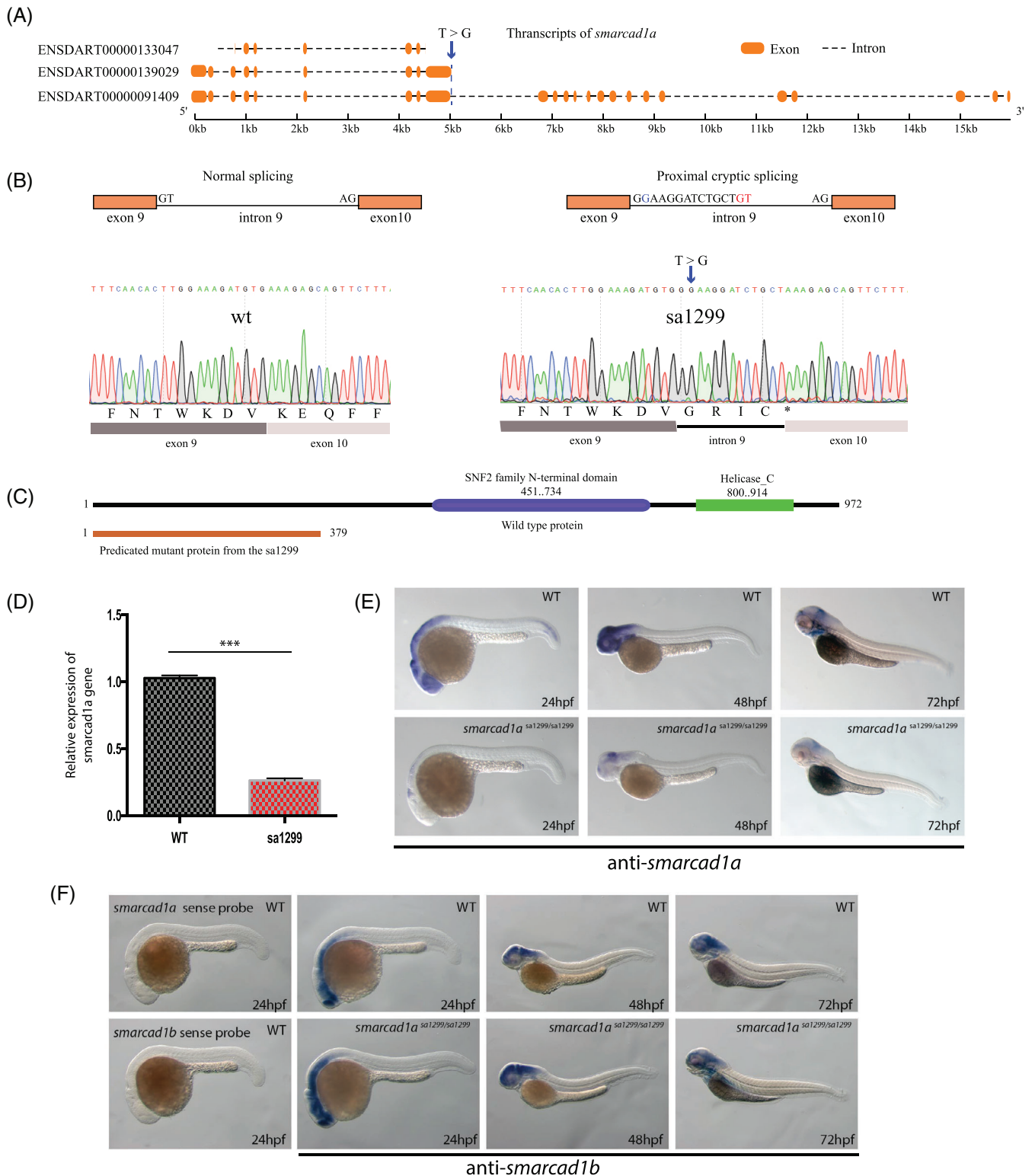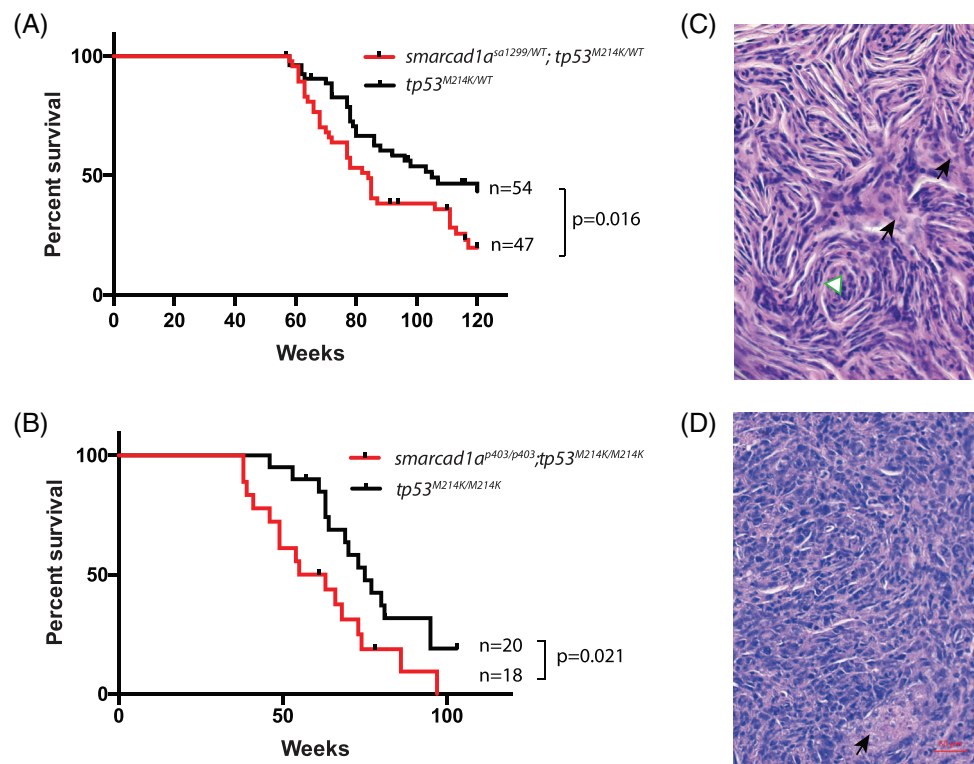

FIGURE 4 Legend on next page.

FIGURE 5 *Smarcad1a* was able to accelerate tumorigenesis in a zebrafish MPNST model initiated by loss-of-function *tp53*. (A) Kaplan–Meier survival curve showing tumor-free survival of cohorts of single (black line) and double heterozygotes (red line) derived from *smarcad1a*[sa1299/WT]; *tp53*[M124K/WT] and *tp53*[M124K/WT]. Fish were genotyped by PCR for each relevant mutation at 6–8 weeks of age and housed segregated by genotype. The numbers of fish of each genotype and the *p* values between the *tp53* single heterozygote and the double mutants are shown in the figure. (B) Kaplan–Meier curve showing tumor-free survival of cohorts of single (black line) and double heterozygotes (red line) derived from *smarcad1a*[p403/p403]; *tp53*[M124K/M124K] and *tp53*[M124K/M124K]. (C) Typical histology of zebrafish MPNST by hematoxylin–eosin staining: spindle cells and swirling structure (white triangle). (D) Heterogonous regions without typical spindle cells from the same tumor. Black arrows indicate necrosis

homozygotes. We found this gene is expressed in similar domains with *smarcad1a* (Figure 4F), supporting our hypothesis.

3.5 | Loss of *smarcad1a* in zebrafish accelerates tumorigenesis of MPNSTs

Zebrafish *smarcad1a* is located on the underrepresented chromosome 8 in our zebrafish MPNST CNA analysis (Figure 1A). Thus, we hypothesized that *smarcad1a* is a tumor suppressor gene in this zebrafish. Zebrafish MPNSTs can be initiated by either *tp53* or *ribosomal protein* (*rp*) gene mutations.[25,65] It has been demonstrated that zebrafish MPSNTs mimic

their human counterpart on multiple levels, from histology to transcriptomes.[8,66] We reasoned that loss of *smarcad1a* might cooperate with initiating *tp53* mutations to promote MPNST development in zebrafish through a synthetic genetic effect if *smarcad1a* is a novel tumor suppressor gene. To test this hypothesis, we crossed the sa1299 mutant with the *tp53*[M214K] zebrafish line. As we expected, double heterozygotes (*smarcad1a*[sa1299/wt]; *tp53*[M214K/wt]) developed MPNST tumors significantly faster than the sibling single heterozygotes (*tp53*[M214K/wt]) (Figure 5A). However, we did not observe tumors from the *smarca1a*[sa1299/wt] heterozygous fish in the same time window, implying that the tumor suppressor function of *smarcad1a* is relatively weak compared to the *tp53* gene. We also did not detect tumor spectrum shift like the zebrafish *reck* gene,[67] and

FIGURE 4 Sa1299 is an essential splicing mutant of the *smarcad1a* gene in zebrafish. (A) Schematic illustration of *smarcad1a* transcription and T to G single nucleotide mutation in the 5′ end essential spicing site of intron 9. The transcription information is based on the GRCz10 in Ensembl. (B) Normal and aberrant splicing are illustrated in the top row. Proximal cryptic splicing resulted in 13 bps from intron 9 retained in the mRNA. T > G mutation is highlighted blue, and cryptic GT is highlighted with red letters. This result was confirmed by Sanger sequencing (bottom row). (C) Predicted functional domains from full-length protein and truncated proteins (without the functional domains) resulted from premature stop codon (asterisk) due to the proximal cryptic splicing. Amino acid numbers are indicated in the diagram. (D) The mRNA level of ENSDART00000091409 is decreased by RT-PCR in 1dpf sa1299 homozygous embryos, most likely caused by nonsense-mediated mRNA decay. (E) Decrease of *smarcad1a* ENSDART00000091409 mRNA also is detected by whole-mount in situ hybridization in 1–3 dpf zebrafish embryos. (F) The *smarcad1b* gene is not affected and still expressed in similar expression domains with *smarcad1a* in sa1299 homozygotes. The sense probe controls are included in the first two vertical panels
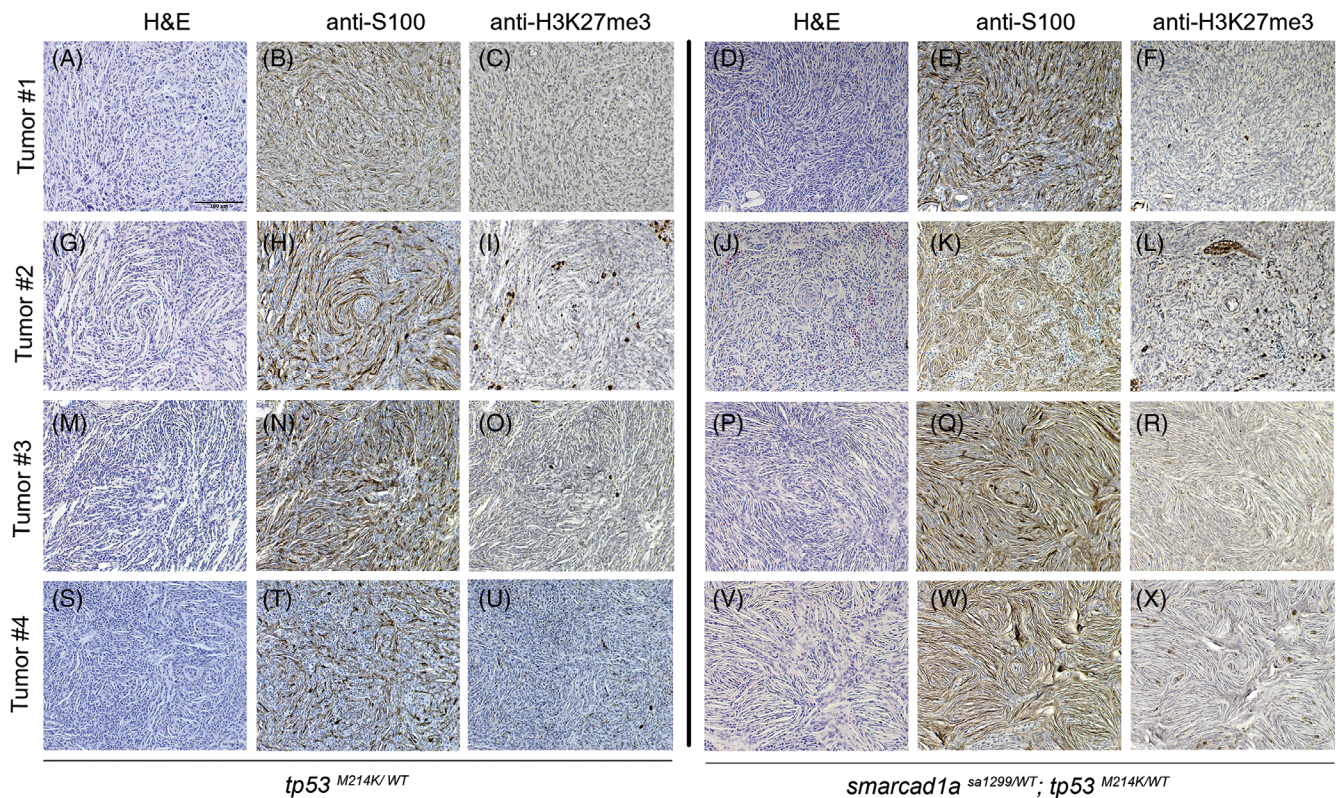
FIGURE 6 Confirmation of zebrafish MPNSTs with S100 and H3K27me3. Four random tumors from *tp53* heterozygotes and double heterozygotes (*tp53* and sa1299) were stained with S100 and H3K27me3 antibodies. (A–C, G–I, M–O, S–U): *tp53* heterozygotes. (D–F, J–L, P–R, V–X): double heterozygotes. HE (hematoxylin and eosin) staining: A, D, G, J, M, P, S, V. IHC with S100 antibody: B, E, H, K, N, Q, T, W. IHC with H3K27me antibody staining: C, F, I, L, O, R, U, X. Some stained cells are non-Schwann cells in these sections, but they serve as a positive control for the antibody specificity. All the images were taken at the same magnification. Scale bar = 100 μm in panel A

all the tumors are MPNSTs. To confirm the identity of MPNSTs, we examined human MPNST markers S100 and H3K27me3 in 4 tumors of *tp53*[M214K/wt] and *smarcad1a*[sa1299/wt]; *tp53*[M214K/wt], respectively. All these tumors are stained with S100, but not H3K27me (Figure 6). These results are consistent with previous reports that zebrafish MPNSTs have high S100 expression[68] and human MPNSTs loss of H3K27me3 expression.[69]

To further confirm the tumor suppressor roles of the *smarcad1a* gene, we created another *smarcad1a* loss-of-function mutant, *smarcad1a*[p403], by using CRISPR technology. We targeted exons 3 and 4 to disrupt all the 3 known zebrafish mRNA transcripts using two CRISPR gRNAs (Figure 7A). One of the knockout mutant lines, p403, deleted 258 bps and gained a 15 bp insertion. Thus, this mutation yielded a truncated protein (about 55–58 amino acids) by introducing a premature stop codon (Figure 7B,C). Like the sa1299 mutant, the homozygous p403 fish could grow to adulthood without any apparent morphological defects. Furthermore, this *smarcad1a*[p403] mutant also showed accelerated tumorigenesis in the *tp53* null background (Figure 5B). Histologically, the tumors from the p403 mutant are similar to those from the sa1299 mutant; both possess the typical spindle cell characteristics and tumor cell morphological heterogeneity (Figure 5C,D). In addition, we did not notice any morphological difference between tumors from both *tp53* heterozygotes and homozygotes, consistent with our past studies.[8,66]

3.6 | DNA damage repair is compromised in zebrafish *smarcad1a* mutants

The yeast *SMARCAD1* homologous gene, *Fun30*, was reported to be required for end resection in the process of DNA DSB repair.[33-35] Recently, *SMARCAD1* was reported to be involved in DNA DSB repair by reducing homologous recombination in an ATM-dependent manner and the mismatch repair (MMR) system, which is mediated by the Msh2 gene[38] in human and *Xenopus* cells, respectively. It has been demonstrated that phosphorylated H2AX (pH2AX) foci duration is elongated in *SMARCAD1* depleted cells. In addition, phosphorylated RPA, 53BP1, BRCA1, and RAD51 foci were decreased in SMARCAD1 depleted cells.[36] Moreover, DNA DSB repair deficiency was also confirmed in human primary fibroblasts and keratinocytes by phosphorylated pH2AX after DSB DNA damage was induced by irradiation.[43] As DNA damage repair is an essential pathway for tumorigenesis, we hypothesize that the zebrafish *smarcad1a* mutant, sa1299, might have DNA damage repair defects. Since pH2AX Ser139 was used as a rough readout of DNA damage repair efficiency,[33,36,43] we chose to examine pH2AX Ser139 in our experiments. If the DNA damage repair machinery is compromised, the presence/duration of pH2AX will be elongated. To test this hypothesis, we treated 1dpf wildtype and sa1299 mutant fish embryos with X-ray irradiation and examined the expression of pH2AX level after irradiation. Indeed, the level
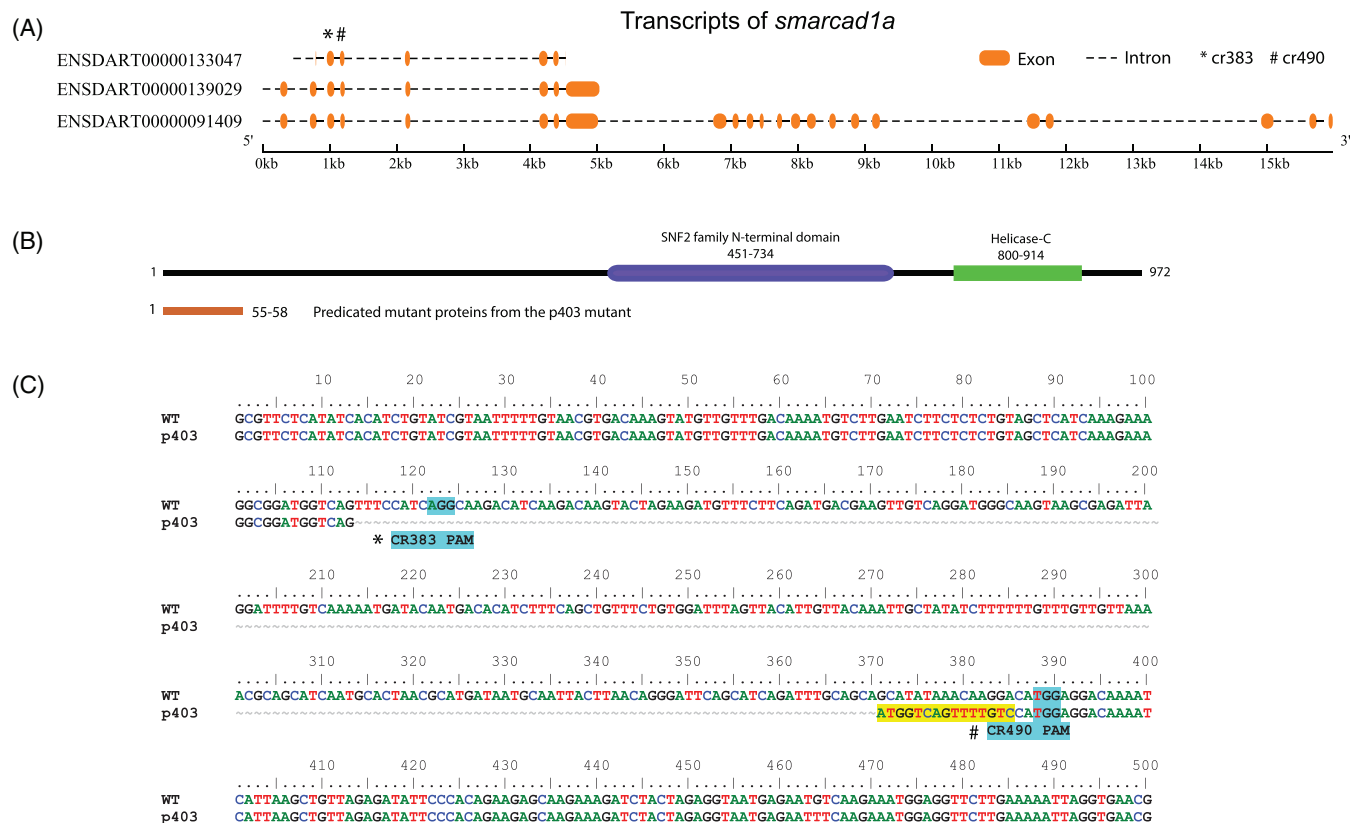
FIGURE 7 Zebrafish *smarcad1a* mutant created by CRISPR. (A) Transcripts of the *smarcad1a* gene, according to Ensembl (GRCz11). (B) Diagram of consequences of the p403 mutant on the SMARCAD1A protein. The top is the intact protein, and the bottom is the truncated protein. Protein domains were predicted by SMART domain. (C) Sequencing result of the *smarcad1a* p403 allele compared with wildtype (WT). The PAMs were highlighted in cyan, and the positions of CRISPR gRNAs are underneath the PAM sequences. The yellow highlighted nucleotides are the insertion. There is a 329 bps deletion from position 114 to 382 in the diagram. The tildes (∼) represent deleted sequences. Asterisk (*) and hashtag (#) indicate the gRNA CR383 and CR490, respectively

of pH2AX decreased slower in both sa1299 and p403, compared to wildtype during the process of recovery after irradiation (Figure 8A,B). This suggests that the DNA damage repairing machinery is compromised in both zebrafish *smarcad1a* mutants.

3.7 | The dosage of *SMARCAD1* is critical for double-strand DNA repair in human neurofibroma and MPNST cells

The *SMARCAD1* gene was found to be involved in the double-strand DNA repair in human U2OS and HeLa cell lines,[33,36] although this remains unknown in MPNST cells. Many DNA damage genes are found to have evolutionarily conserved cellular functions. Thus, based on our results of zebrafish *smarcad1* DNA damage repair defect (Figure 8), we reasoned that human *SMARCAD1* might have similar functions in DNA damage repair in human MPNST cell lines. To test our hypothesis, we first created a tetracycline-inducible *SMARCAD1* knockdown cell line using shRNA in a premalignant neurofibroma cell line, HEI-193 (Figure S4A,B), since it has a relatively high expression (Figure 1F). Then, we

examined the repair of DNA DSBs with these cell lines. We found the level of pH2AX Ser139 diminished slower in the *SMARCAD1* knockdown cells after both 10 and 20 Gy irradiation treatment, comparing to the control cells (Figure 9A,B).

In our zebrafish CNA analysis, *smarcad1a* was underrepresented in more than half of the samples. However, the *smarcad1b* showed the opposite (Figure 1B,C). In addition, *SMARCAD1* amplifications and deletions are also frequently present in some human cancers such as sarcoma and ovarian (Figure 1D). Considering *smarcad1a* and *smarcad1b* have potentially similar functions, we hypothesized that the gene dosage (increase or decrease of gene function) of *SMARCAD1* is imperative for maintaining genomic stability in response to double-strand DNA damage repair. To test this hypothesis in human cells, we created another tetracycline-inducible *SMARCAD1*-overexpressing human MPNST cell line, STS26T (Figure S4C). We choose this cell line because the SMARCAD1 expression is relatively lower than in schwannoma cell HEI-193 (Figure 1F), and it may represent sporadic MPNSTs that are consistent with our zebrafish MPNST model. Indeed, the expression of pH2AX decreased slower after both 10 and 20 Gy X-ray irradiation in doxycycline-treated samples (Figure 9C,D). This result suggests that SMARCAD1 plays a role in
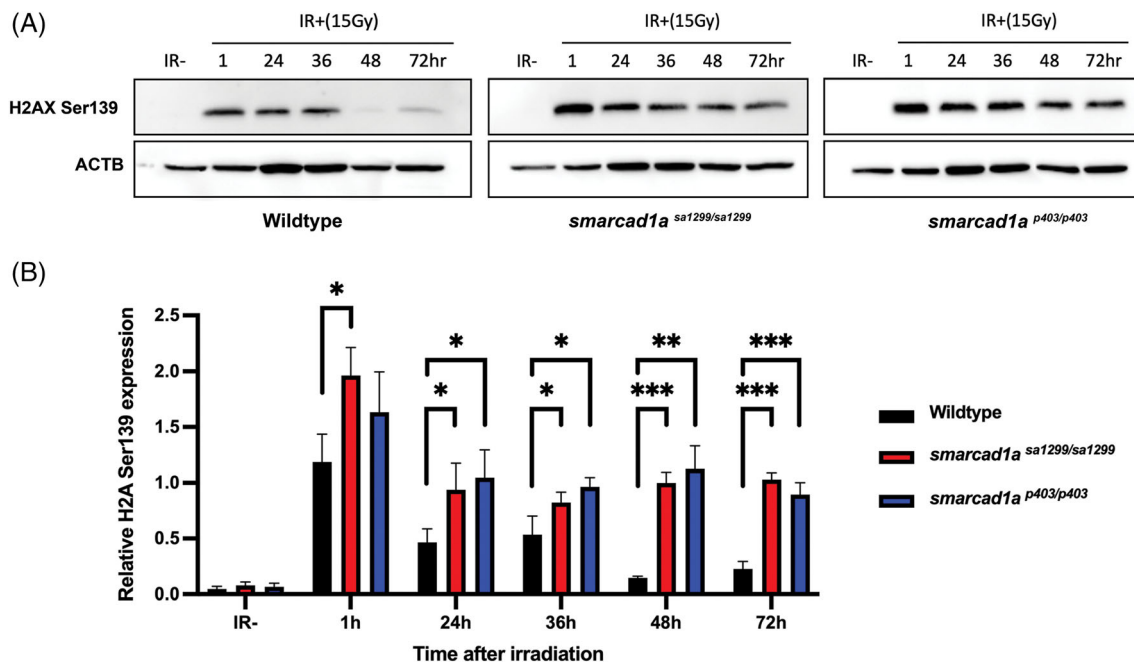
FIGURE 8 DNA damage response is compromised in zebrafish embryos. (A) Representative western blot showing protein expression or phosphorylation of H2AX ser139 upon the indicated treatment in wildtype, $smarcad1a^{sa1299-/-}$, and $smarcad1a^{p403-/-}$ 1dpf zebrafish embryos. For irradiated samples (IR+), samples were harvested at the indicated hour post 15 Gy IR. (B) Quantification of protein expression via western blotting from panel A. For each biological replicate, values were normalized to the value for "IR−" to calculate the fold change in phosphorylation of H2AX upon the indicated treatment. Bars in (B) are the mean of three independent experiments. Statistical analysis comparing experimental to the control ("IR−") was performed using Welch's t test (*$p ≤ 0.05$; **$p ≤ 0.01$; ***$p ≤ 0.001$; ****$p ≤ 0.0001$; NS $p > 0.05$)
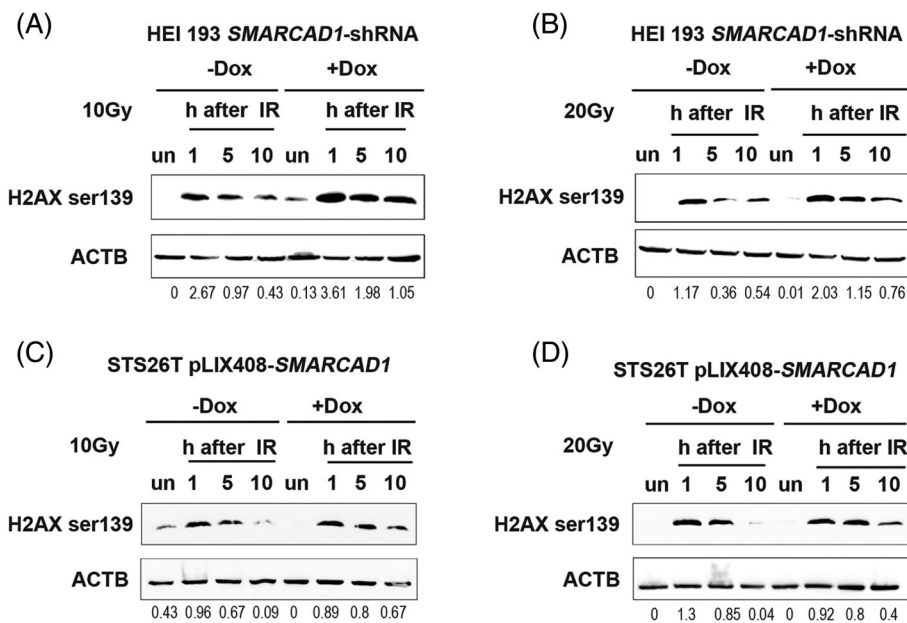

FIGURE 9 Human cells show a defect in double-strand DNA damage repair. (A, B) Double-strand DNA damage repair was measured by Western blots with anti-histone H2AX S139ph (phospho Ser139) in *SMARCAD1* knockdown schwannoma cell line HEI-193 after X-ray irradiations (10 and 20 Gy, respectively). ULTRA-3351712 knockdown cell was used for this experiment. Doxycycline (final concentration: 0.1 μg/ml) was added 48 h ahead of the experiments. (C, D) Double-strand DNA damage repair in *SMARCAD1* overexpression MPNST cells (STS26T) by H2AX S139ph. Doxycycline (final concentration: 1 μg/ml) was added 24 h ahead of the experiments. Both cell lines were harvested at 1, 5, and 10 h post-irradiation along with untreated samples. un, untreated sample. Beta-actin (ACTB) was used as a loading control. The densitometry ratios of H2A X S139ph over ACTB was listed underneath the blots
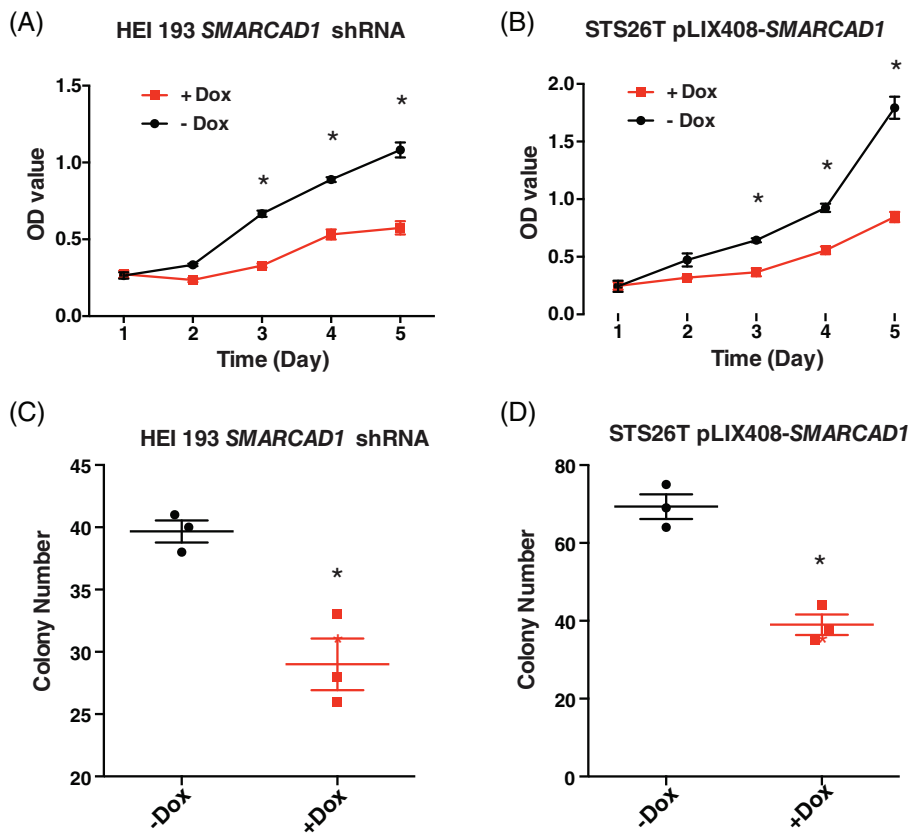
(A)

HEI 193 *SMARCAD1* shRNA

(B)

STS26T pLIX408-*SMARCAD1*

(C)

HEI 193 *SMARCAD1* shRNA

(D)

STS26T pLIX408-*SMARCAD1*

FIGURE 10 Cell proliferation and independent growth were inhibited in both *SMARCAD1* knockdown and overexpression. Proliferation was measured by MTT assay in *SMARCAD1* knockdown HEI193 cells (A) and overexpression STS26T cells (B). Growth differences were evident from day 3 in both cases. Anchorage-independent growth was examined by soft-agar assay in *SMARCAD1* knockdown HEI193 cells (C) and overexpression STS26T cells (D). All the assays were done with three biological replicates. Asterisk (*) indicates statistical significance, $p < 0.05$
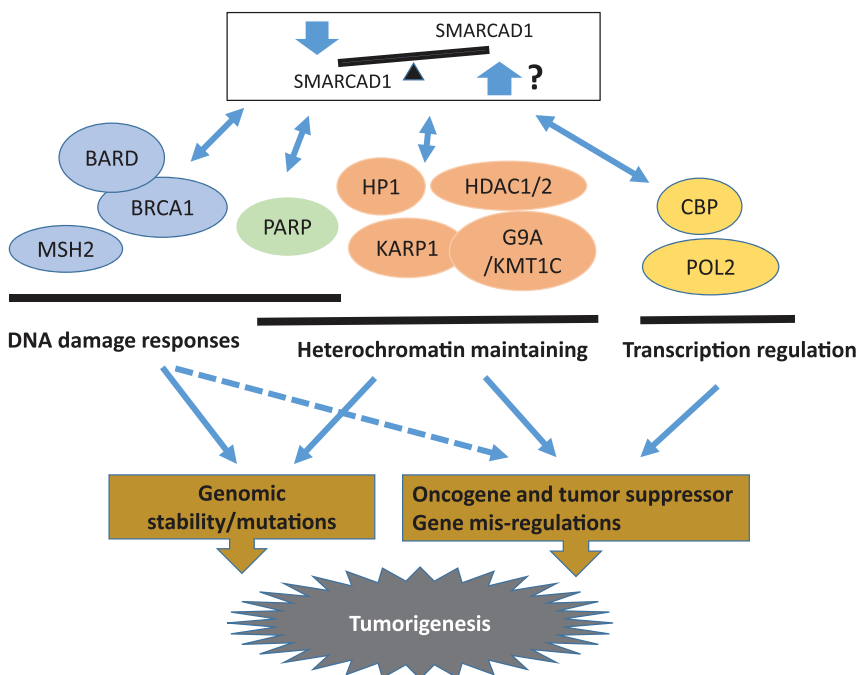

FIGURE 11 Model of SMARCAD1 tumor suppressor mechanisms. Three mechanisms (DNA damage response, heterochromatin maintaining, and transcription regulation) were proposed based on current knowledge.[33,34,36,38,72,73,80,81] The bidirectional arrows indicate protein–protein interactions. The arrows imply cellular consequences. The dashed arrows show a possible result. The involved genes and pathways are solely based on loss-of-function studies due to the lack of overexpression reports

DNA damage repair in a gene dosage-sensitive manner. This dosage sensitivity could be caused by the stoichiometric effect with its partner proteins found in some protein-complex.[70] To further investigate the tumorigenic impacts of *SMARCAD1*, we performed MTT and soft agar colony formation assays in both *SMARCAD1* knockdown and overexpression cell lines. We found that cell growth rate and anchorage-independent growth decreased in both cases (Figure 10A–D). These results suggest that the proper gene dosage or amount of SMARCAD1 protein might be required for maintaining normal cell growth.

4 | DISCUSSION

As cancer is essentially a genetic or genomic disease, one of the goals of current cancer research is to identify cancer driver genes that can be used as targets for cancer therapy and/or markers for diagnosis and prognosis. It remains challenging to identify cancer driver genes on large CNAs or aneuploid chromosomes in the era of massively parallel sequencing technology, simply because they are usually altered as a unit that carries many genes. Unless the cancer driver genes also have point mutations, it is very challenging to tell the driver genes apart from the passenger genes along with the altered chromosome fragments. Here, we focused on one candidate gene, *SMARCAD1*, on human chromosome 4q22-23, due to the prevalence of chromatin remodelers as cancer drivers. We demonstrated that this gene is a *bone fide* tumor suppressor gene in zebrafish MPNSTs. Moreover, our experiments in human MPNST cells suggest that SMARCAD1 is involved in the DNA DSB repairing response in zebrafish embryos and human MPNST cell lines. These results are consistent with previous reports on other human cells.[33,36,43] Given the sensitivity of *SMARCAD1* mutant cells to PARP inhibitors, the demonstration of *smarcad1a* as a tumor suppressor gene might provide a new potential target for MPNST therapy.

4.1 | Loss of *smarcad1a* accelerates MPNST tumorigenesis, suggesting it is a novel tumor suppressor gene in zebrafish

The *SMARCAD1* gene encodes a member of the SWI/SNF (switching defective/sucrose non-fermenting) complex, a well-characterized machinery that affects chromatin structure that is frequently mutated in many human cancers.[29,30,71,72] The yeast orthologous *FUN30/FFT3* has been found to play essential roles in regulating and maintaining silent chromatin domains, repairing DNA DSBs, preserving genome stability, and facilitating polymerase II transcriptional elongation.[33,34,36,43,72,73] However, until now, there was no clear in vivo evidence to support that *SMARCAD1* is a tumor suppressor gene. Here, we report the first in vivo genetic evidence that the zebrafish *smarcad1a* gene is a novel tumor suppressor gene, as both sa1299 and p403 mutant fish showed increase tumorigenesis with *tp53* mutant-initiated MNPSTs. Furthermore, we have demonstrated that double-strand DNA break repair is compromised in both mutants, suggesting that *smarcad1a* is required to maintain genomic integrity. Thus, defects in DNA repair upon the misregulation of this gene may be one of its tumorigenic mechanisms. In the future, it will be interesting to investigate the mechanistic role of *smarcad1* genes in DNA damage repair pathways *in vivo* using zebrafish models. In addition, it is worth noting that *Smarcad1* null mice were reported to die from gastrointestinal tumors, although the skeletal defects were the primary phenotype in live mice from an early knockout mouse study.[74] Along this line, human *SMARCAD1* mutations were found to cause Huriez syndrome (sclerotylosis), Basan syndrome (adermatoglyphia), and are susceptible to skin cancers.[36,75] Altogether, these data

suggest that *SMARCAD1* may be an evolutionarily conserved tumor suppressor gene in vertebrates. Future conditional knockout mouse models will be helpful to address whether *Smarcad1* is also involved in mouse MPNSTs since the new conditional mice were just created recently.[76]

In our experiments, both SMRACAD1 knockdown in HEI-193 and overexpression in STS26T led to cell growth inhibition. This phenomenon may be due to more SMARCAD1 protein than physiologically needed, leading to lengthened resection tracks, which would also be deleterious to genome stability and indirectly cause cell growth inhibition. Thus, as tumor suppressor gene involved in DNA damage repair, either gain or loss of function may lead to cellular misfunction, similar to BRCA1 and BRCA2. The knockout of *Brca1* and *Brca2* resulted in embryonic lethality and cell proliferation defects in mice,[77] while overexpression of *BRCA1* and *BRCA2* also causes anti-proliferative effects in human cells.[78,79] This could be a common feature of tumor suppressor genes that are all involved in DNA damage repair. Therefore, we should not exclude *SMARCAD1* as a tumor suppressor because the knockdown of this gene in human cells slows cell growth. Since both STS26T and HEI-193 are not NF1 mutants, it will be informative to examine NF1 mutant Schwann cell lines and NF1-related MPNSTs in the future since the schwannoma cell HEI-193 possesses an NF2 mutation.

For the molecular mechanism of *smarcad1a* as a tumor suppressor, there could be a few possibilities. First, SMARCAD1 and its orthologues were repeatedly reported to be essential for DNA damage repair in yeast and human cell lines.[33,34,36] It was known that BRCA1-BARD1's function in homologous recombination requires SMARCAD1.[80] In addition, SMARCAD1 is required by Msh2 for mismatch repairs.[38] Our pH2AX expression results of zebrafish embryos, human neurofibroma, and MPNST cells after irradiation support that this gene is needed for DNA damage repair, although the detailed roles in different repair pathways need further investigation. Second, SMARCAD1 was reported to play important roles in maintaining genome stability through heterochromatin silencing, endogenous retrovirus inhibition, interacting with E1a oncoprotein, and replication fork stability.[21,39,40,72] Third, as a chromatin remodeler, SMARCAD1 was also reported to regulate gene expression through transcription.[81,82] Another chromatin remodeler, SMARCB1/INI1 was reported to regulate RB1, MYC, SHH, and WNT signaling pathways.[83] Thus, SMARCAD1 mutation or misexpression may directly lead to other oncogene activation and tumor suppressor gene inactivation, which may cause cancer. Based on these possibilities, we propose a model of *SMARCAD1* as a tumor suppressor in Figure 11.

4.2 | Developmental roles of *SMARCAD1*

Mouse *Smarcad1* (a.k.a. *Etl1*) was first reported from a LacZ enhancer trap line. It was expressed in the central nervous system, mesenchyme of the maxillary and mandibular arches, limb bud ectodermal cells around the snout and limb buds, liver, and spinal ganglia of mouse embryos.[84] The mouse neural expression is similar to what we found

in zebrafish embryos, suggesting its roles during neural development are evolutionarily conserved. *Smarcad1* loss-of-function mice were created through recombination by inserting a selectable marker (lacZ-neo or hygromycin B-phosphotransferase) in frame to the *Smarcad1* coding sequence immediately downstream of the first ATG to preclude the generation of any full-length protein.[74] About half of the homozygous *Smarcad1* inactivated mice (48%) were able to survive to adulthood but exhibited variable skeletal dysplasia and reduced body weight.[74] It is worth mentioning that gastrointestinal tumors were noticed in some of the lost homozygous mutants by autopsy.[74] In contrast, our zebrafish *smarcad1a* sa2199 and p403 adult homozygotes did not have any noticeable morphological abnormalities or postnatal mortality. One likely explanation is the functional gene compensation. This idea is supported by the zebrafish *smarcad1a* and *smarcad1b* genes sharing overlapped expression during embryogenesis (Figure 3), as well as *smarcad1b* expression not being affected in the sa1299 null mutant embryos (Figure 4F). Future studies with the inactivation of the *smarcad1b* gene will be interesting to test this possibility.

In humans, *SMARCAD1* gene mutants and variants were reported to be linked to Basan syndrome, an autosomal-dominant adermatoglyphia, which is characterized by rapid healing congenital acral bullae, congenital milia, and lack of fingerprints.[42,85] In addition, SMARCAD1 was also linked to a rare dominant disease, Huriez syndrome, which is characterized by congenital palmoplantar keratosis, scleroatrophic changes of the hands and feet, and an increased risk for cutaneous squamous cell carcinoma.[43] Detailed examination of zebrafish or mouse embryonic development might shed light on these specific genetic diseases in humans.

4.3 | Cellular functions of SMARCAD1 and future cancer therapy development

SMARCAD1 is a member of the SNF2 helicase subfamily. The members of this subfamily, such as *ION80* and *SWR1* genes, are known to play essential roles in the DNA damage repair processes.[86,87] Here, we have confirmed this DNA damage repair function in zebrafish *smarcad1a* mutants and human MPNST cell lines. More importantly, we demonstrated that the dosage of this gene, either overexpressed or downregulated, is critical for DNA DSB responses induced by X-ray irradiation. The sensitivity of *SMARCAD1* mutant cancer cells to DNA enzyme topoisomerase I inhibitor, CPT (camptothecin), and PARP inhibitors is beneficial for developing new therapies for MPNSTs given there is no effective treatment for this type of malignancy.[12] Similar to *BRCA1* and *BRCA2* genes, the *SMARCAD1* gene is also involved in the DNA end-resection process and interacts with KAP1, BRCA1, and PARP1.[72,80] Thus, this gene might provide us another targetable tumor suppresser gene with PARP inhibitors. Although we demonstrated the tumor suppressor activity of *smarcad1a* in MPNSTs here, its potential application with PARP inhibitors should not be limited to this type of cancer. This is evident with the *SMARCAD1*-knockdown osteosarcoma cell line, U2OS, which showed a similar response to CPT and PARP inhibitors.[33] Of course, this idea needs more experimental support and SMARCAD1 mutation characterization

from human MPNST studies. There is still a long way to go to prove this idea.

Interestingly, human *SMARCAD1* variants were also reported to be correlated with fluorouracil (5-FU) sensitivity by GWAS, suggesting that *SMARCAD1* might also be a useful marker for cancer treatment decisions.[88] Additionally, it is worth noting that homozygous *Smarcad1* mouse mutant embryonic stem cells did not show differences in their survival rates after gamma or UV-radiation treatment.[74] However, consistent evidence from yeast, zebrafish, and human cells suggests DNA damage repair is an evolutionarily conserved function of *SMARCAD1*. One possible explanation for this difference could be incomplete inactivation of the mouse *Smarcad1* gene (a.k.a. *ETL1*), or irradiation dosage threshold. Future studies with *Smarcad1* are needed to clarify the discrepancy with the reported mouse mutant.

4.4 | Future of zebrafish–human comparative cancer genomics and the zebrafish cancer model

Cross-species comparative oncogenomics serves as one of the solutions for identifying cancer drivers on large CNAs due to genes conserved functions.[5-8] We have found that zebrafish–human comparative cancer genomics with CNAs is an effective way to narrow down the cancer driver candidate genes on aneuploid chromosomes.[8,66] In this report, we demonstrated that the *smarcad1*a mutants, sa1299 and p403, accelerated tumorigenesis initiated by *tp53*. Thus, *smarcad1a* is a novel tumor suppressor gene in zebrafish MPNSTs. Moreover, our results also demonstrated that the combination of zebrafish–human comparative cancer genomics and functional genetic studies in zebrafish is a powerful approach for a long-lasting challenge for identifying novel cancer driver genes on large CNAs/aneuploid chromosomes. Considering the plethora of available zebrafish mutants from large-scale forward genetic screens and convenient reverse genetics, such as TALEN and CRISPR,[89-92] a relatively large number of candidate cancer driver genes can be functionally validated in vivo with a similar approach as demonstrated for the *smarcad1a* gene here.

CONFLICT OF INTEREST
All authors declare no conflict of interest.

AUTHOR CONTRIBUTIONS
GuangJun Zhang designed the project and coordinated research; Han Han, Guangzhen Jiang, Rashmi Kumari, Martin R. Silic, Jake L. Owens,

DATA AVAILABILITY STATEMENT

ORCID

Han Han https://orcid.org/0000-0002-8479-8472
Guangzhen Jiang https://orcid.org/0000-0002-4608-0267
Martin R. Silic https://orcid.org/0000-0003-3433-3922
Jake L. Owens https://orcid.org/0000-0002-7359-5338
GuangJun Zhang https://orcid.org/0000-0002-0839-5161

REFERENCES

1. Gatenby RA. A change of strategy in the war on cancer. *Nature*. 2009; 459(7246):508-509.
2. Stratton MR, Campbell PJ, Futreal PA. The cancer genome. *Nature*. 2009;458(7239):719-724.
3. Cowin PA, Anglesio M, Etemadmoghadam D, Bowtell DD. Profiling the cancer genome. *Annu Rev Genomics Hum Genet*. 2010;11:133-159.
4. Beroukhim R, Mermel CH, Porter D, et al. The landscape of somatic copy-number alteration across human cancers. *Nature*. 2010;463 (7283):899-905.
5. Zhang G, Vemulapalli TH, Yang JY. Phylooncogenomics: examining the cancer genome in the context of vertebrate evolution. *Appl Transl Genom*. 2013;2:48-54.
6. Maser RS, Choudhury B, Campbell PJ, et al. Chromosomally unstable mouse tumours have genomic alterations similar to diverse human cancers. *Nature*. 2007;447(7147):966-971.
7. Tang J, Le S, Sun L, et al. Copy number abnormalities in sporadic canine colorectal cancers. *Genome Res*. 2010;20(3):341-350.
8. Zhang G, Hoersch S, Amsterdam A, et al. Comparative oncogenomic analysis of copy number alterations in human and zebrafish tumors enables cancer driver discovery. *PLoS Genet*. 2013;9(8):e1003734.
9. Ng VY, Scharschmidt TJ, Mayerson JL, Fisher JL. Incidence and survival in sarcoma in the United States: a focus on musculoskeletal lesions. *Anticancer Res*. 2013;33(6):2597-2604.
10. Ducatman BS, Scheithauer BW, Piepgras DG, Reiman HM, Ilstrup DM. Malignant peripheral nerve sheath tumors. A clinicopathologic study of 120 cases. *Cancer*. 1986;57(10):2006-2021.
11. Kolberg M, Holand M, Agesen TH, et al. Survival meta-analyses for >1800 malignant peripheral nerve sheath tumor patients with and without neurofibromatosis type 1. *Neuro Oncol*. 2013;15(2):135-147. https://doi.org/10.1093/neuonc/nos287.
12. Durbin AD, Ki DH, He S, Look AT. Malignant peripheral nerve sheath tumors. *Adv Exp Med Biol*. 2016;916:495-530.
13. Beert E, Brems H, Daniels B, et al. Atypical neurofibromas in neurofibromatosis type 1 are premalignant tumors. *Genes Chromosomes Cancer*. 2011;50(12):1021-1032. https://doi.org/10.1002/gcc.20921.
14. Cetin E, Cengiz B, Gunduz E, et al. Deletion mapping of chromosome 4q22-35 and identification of four frequently deleted regions in head and neck cancers. *Neoplasma*. 2008;55(4):299-304.
15. Uzunoglu FG, Dethlefsen E, Hanssen A, et al. Loss of 4q21.23-22.1 is a prognostic marker for disease free and overall survival in non-small cell lung cancer. *PLoS One*. 2014;9(12):e113315.
16. Xu Y, Man XH, Lv Z, et al. Loss of heterozygosity at chromosomes 1p35-pter, 4q, and 18q and protein expression differences between adenocarcinomas of the distal stomach and gastric cardia. *Hum Pathol*. 2012;43(12):2308-2317.
17. Brosens RPM, Belt EJTH, Haan JC, et al. Deletion of chromosome 4q predicts outcome in stage II colon cancer patients. *Cell Oncol*. 2011; 34(3):215-223.
18. Shinno Y, Gunduz E, Gunduz M, et al. Fine deletional mapping of chromosome 4q22-35 region in oral cancer. *Int J Mol Med*. 2005;16 (1):93-98.
19. Rozier L, El-Achkar E, Apiou F, Debatisse M. Characterization of a conserved aphidicolin-sensitive common fragile site at human 4q22 and mouse 6C1: possible association with an inherited disease and cancer. *Oncogene*. 2004;23(41):6872-6880.
20. Sud A, Cooke R, Swerdlow AJ, Houlston RS. Genome-wide homozygosity signature and risk of Hodgkin lymphoma. *Sci Rep*. 2015;5: 14315.
21. Adra CN, Donato JL, Badovinac R, et al. SMARCAD1, a novel human helicase family-defining member associated with genetic instability: cloning, expression, and mapping to 4q22-q23, a band rich in breakpoints and deletion mutants involved in several human diseases. *Genomics*. 2000;69(2):162-173.
22. Mione MC, Trede NS. The zebrafish as a model for cancer. *Dis Model Mech*. 2010;3(9-10):517-523.
23. Langenau DM, Traver D, Ferrando AA, et al. Myc-induced T cell leukemia in transgenic zebrafish. *Science*. 2003;299(5608):887-890.
24. Langenau DM, Keefe MD, Storer NY, et al. Effects of RAS on the genesis of embryonal rhabdomyosarcoma. *Genes Dev*. 2007;21(11):1382-1395.
25. Berghmans S, Murphey RD, Wienholds E, et al. tp53 mutant zebrafish develop malignant peripheral nerve sheath tumors. *Proc Natl Acad Sci U S A*. 2005;102(2):407-412.
26. Patton EE, Widlund HR, Kutok JL, et al. BRAF mutations are sufficient to promote nevi formation and cooperate with p53 in the genesis of melanoma. *Curr Biol*. 2005;15(3):249-254.
27. Faucherre A, Taylor GS, Overvoorde J, Dixon JE, Hertog J. Zebrafish pten genes have overlapping and non-redundant functions in tumorigenesis and embryonic development. *Oncogene*. 2008;27(8):1079-1086.
28. Centore RC, Sandoval GJ, Soares LMM, Kadoch C, Chan HM. Mammalian SWI/SNF chromatin remodeling complexes: emerging mechanisms and therapeutic strategies. *Trends Genet*. 2020;36(12):936-950.
29. Kadoch C, Crabtree GR. Mammalian SWI/SNF chromatin remodeling complexes and cancer: mechanistic insights gained from human genomics. *Sci Adv*. 2015;1(5):e1500447.
30. Roberts CW, Orkin SH. The SWI/SNF complex—chromatin and cancer. *Nat Rev Cancer*. 2004;4(2):133-142. https://doi.org/10.1038/nrc1273.
31. Pemov A, Hansen NF, Sindiri S, et al. Low mutation burden and frequent loss of CDKN2A/B and SMARCA2, but not PRC2, define premalignant neurofibromatosis type 1-associated atypical neurofibromas. *Neuro Oncol*. 2019;21(8):981-992.
32. Flaus A, Martin DM, Barton GJ, Owen-Hughes T. Identification of multiple distinct Snf2 subfamilies with conserved structural motifs. *Nucleic Acids Res*. 2006;34(10):2887-2905.
33. Costelloe T, Louge R, Tomimatsu N, et al. The yeast Fun30 and human SMARCAD1 chromatin remodellers promote DNA end resection. *Nature*. 2012;489(7417):581-584.
34. Chen X, Cui D, Papusha A, et al. The Fun30 nucleosome remodeller promotes resection of DNA double-strand break ends. *Nature*. 2012; 489(7417):576-580.

35. Neves-Costa A, Will WR, Vetter AT, Miller JR, Varga-Weisz P. The SNF2-family member Fun30 promotes gene silencing in heterochromatic loci. *PLoS One*. 2009;4(12):e8111.

36. Chakraborty S, Pandita RK, Hambarde S, et al. SMARCAD1 phosphorylation and ubiquitination are required for resection during DNA double-strand break repair. *iScience*. 2018;2:123-135.

37. Ouspenski II, Elledge SJ, Brinkley BR. New yeast genes important for chromosome integrity and segregation identified by dosage effects on genome stability. *Nucleic Acids Res*. 1999;27(15):3001-3008.

38. Terui R, Nagao K, Kawasoe Y, et al. Nucleosomes around a mismatched base pair are excluded via an Msh2-dependent reaction with the aid of SNF2 family ATPase Smarcad1. *Genes Dev*. 2018;32(11-12):806-821.

39. Sachs P, Ding D, Bergmaier P, et al. SMARCAD1 ATPase activity is required to silence endogenous retroviruses in embryonic stem cells. *Nat Commun*. 2019;10(1):1335.

40. Lo CSY, van Toorn M, Gaggioli V, et al. SMARCAD1-mediated active replication fork stability maintains genome integrity. *Sci Adv*. 2021;7(19):eabe7804.

41. Valentin MN, Solomon BD, Richard G, Ferreira CR, Kirkorian AY. Basan gets a new fingerprint: mutations in the skin-specific isoform of SMARCAD1 cause ectodermal dysplasia syndromes with adermatoglyphia. *Am J Med Genet A*. 2018;176(11):2451-2455.

42. Li M, Wang J, Li Z, et al. Genome-wide linkage analysis and whole-genome sequencing identify a recurrent SMARCAD1 variant in a unique Chinese family with Basan syndrome. *Eur J Hum Genet*. 2016;24(9):1367-1370.

43. Gunther C, Lee-Kirsch MA, Eckhard J, et al. SMARCAD1 haploinsufficiency underlies Huriez syndrome and associated skin cancer susceptibility. *J Invest Dermatol*. 2018;138(6):1428-1431.

44. Westerfield M. *The Zebrafish Book. A Guide for the Laboratory Use of Zebrafish (Danio Rerio)*. 4th ed. Eugene: University of Oregon Press; 2000. https://zfin.org/zf_info/zfbook/zfbk.html.

45. Truett GE, Heeger P, Mynatt RL, Truett AA, Walker JA, Warman ML. Preparation of PCR-quality mouse genomic DNA with hot sodium hydroxide and tris (HotSHOT). *Biotechniques*. 2000;29(1):52-54.

46. Hwang WY, Fu Y, Reyon D, et al. Efficient genome editing in zebrafish using a CRISPR-Cas system. *Nat Biotechnol*. 2013;31(3):227-229.

47. Silic MR, Zhang G. Visualization of cellular electrical activity in zebrafish early embryos and tumors. *J Vis Exp*. 2018;134:57330.

48. Livak KJ, Schmittgen TD. Analysis of relative gene expression data using real-time quantitative PCR and the 2(T)(-Delta Delta C) method. *Methods*. 2001;25(4):402-408. https://doi.org/10.1006/meth.2001.1262.

49. Edgar RC. MUSCLE: multiple sequence alignment with high accuracy and high throughput. *Nucleic Acids Res*. 2004;32(5):1792-1797.

50. Tamura K, Stecher G, Peterson D, Filipski A, Kumar S. MEGA6: molecular evolutionary genetics analysis version 6.0. *Mol Biol Evol*. 2013;30(12):2725-2729.

51. Guindon S, Dufayard JF, Lefort V, Anisimova M, Hordijk W, Gascuel O. New algorithms and methods to estimate maximum-likelihood phylogenies: assessing the performance of PhyML 3.0. *Syst Biol*. 2010;59(3):307-321.

52. Catchen JM, Conery JS, Postlethwait JH. Automated identification of conserved synteny after whole-genome duplication. *Genome Res*. 2009;19(8):1497-1505.

53. Letunic I, Bork P. 20 years of the SMART protein domain annotation resource. *Nucleic Acids Res*. 2018;46(D1):D493-D496.

54. Hensley MR, Cui Z, Chua RF, et al. Evolutionary and developmental analysis reveals KANK genes were co-opted for vertebrate vascular development. *Sci Rep*. 2016;6:27816.

55. Hensley MR, Chua RF, Leung YF, Yang JY, Zhang G. Molecular evolution of MDM1, a "duplication-resistant" gene in vertebrates. *PLoS One*. 2016;11(9):e0163229.

56. Cui Z, Shen Y, Chen KH, Mittal SK, Yang JY, Zhang G. KANK1 inhibits cell growth by inducing apoptosis through regulating CXXC5 in human malignant peripheral nerve sheath tumors. *Sci Rep*. 2017;7:40325.

57. Gao JJ, Aksoy BA, Dogrusoz U, et al. Integrative analysis of complex cancer genomics and clinical profiles using the cBioPortal. *Sci Signal*. 2013;6(269):pl1.

58. Jaillon O, Aury JM, Brunet F, et al. Genome duplication in the teleost fish *Tetraodon nigroviridis* reveals the early vertebrate proto-karyotype. *Nature*. 2004;431(7011):946-957.

59. Angel Amores AF, Yan Y-L, Joly L, et al. Zebrafish hox clusters and vertebrate genome evolution. *Science*. 1998;282:1711-1714. https://science.sciencemag.org/content/282/5394/1711.long.

60. Taylor JS, Braasch I, Frickey T, Meyer A, Van de Peer Y. Genome duplication, a trait shared by 22000 species of ray-finned fish. *Genome Res*. 2003;13(3):382-390.

61. Force A, Lynch M, Pickett FB, Amores A, Yan YL, Postlethwait J. Preservation of duplicate genes by complementary, degenerative mutations. *Genetics*. 1999;151(4):1531-1545.

62. Kettleborough RN, Busch-Nentwich EM, Harvey SA, et al. A systematic genome-wide analysis of zebrafish protein-coding gene function. *Nature*. 2013;496(7446):494-497.

63. Lykke-Andersen S, Jensen TH. Nonsense-mediated mRNA decay: an intricate machinery that shapes transcriptomes. *Nat Rev Mol Cell Biol*. 2015;16(11):665-677.

64. Brogna S, Wen J. Nonsense-mediated mRNA decay (NMD) mechanisms. *Nat Struct Mol Biol*. 2009;16(2):107-113.

65. Amsterdam A, Sadler KC, Lai K, et al. Many ribosomal protein genes are cancer genes in zebrafish. *PLoS Biol*. 2004;2(5):E139.

66. Zhang G, Hoersch S, Amsterdam A, Whittaker CA, Lees JA, Hopkins N. Highly aneuploid zebrafish malignant peripheral nerve sheath tumors have genetic alterations similar to human cancers. *Proc Natl Acad Sci U S A*. 2010;107(39):16940-16945.

67. Kumari R, Silic MR, Jones-Hall YL, et al. Identification of RECK as an evolutionarily conserved tumor suppressor gene for zebrafish malignant peripheral nerve sheath tumors. *Oncotarget*. 2018;9(34):23494-23504.

68. White LA, Sexton JM, Shive HR. Histologic and immunohistochemical analyses of soft tissue sarcomas from brca2-mutant/tp53-mutant zebrafish are consistent with neural crest (Schwann cell) origin. *Vet Pathol*. 2017;54(2):320-327.

69. Prieto-Granada CN, Wiesner T, Messina JL, Jungbluth AA, Chi P, Antonescu CR. Loss of H3K27me3 expression is a highly sensitive marker for sporadic and radiation-induced MPNST. *Am J Surg Pathol*. 2016;40(4):479-489.

70. Taggart JC, Li GW. Production of protein-complex components is stoichiometric and lacks general feedback regulation in eukaryotes. *Cell Syst*. 2018;7(6):580-589.e4.

71. Stralfors A, Walfridsson J, Bhuiyan H, Ekwall K. The FUN30 chromatin remodeler, Fft3, protects centromeric and subtelomeric domains from euchromatin formation. *PLoS Genet*. 2011;7(3):e1001334.

72. Rowbotham SP, Barki L, Neves-Costa A, et al. Maintenance of silent chromatin through replication requires SWI/SNF-like chromatin remodeler SMARCAD1. *Mol Cell*. 2011;42(3):285-296.

73. Lee J, Choi ES, Seo HD, et al. Chromatin remodeller Fun30Fft3 induces nucleosome disassembly to facilitate RNA polymerase II elongation. *Nat Commun*. 2017;8:14527.

74. Schoor M, Schuster-Gossler K, Roopenian D, Gossler A. Skeletal dysplasias, growth retardation, reduced postnatal survival, and impaired fertility in mice lacking the SNF2/SWI2 family member ETL1. *Mech Dev*. 1999;85(1-2):73-83.

75. Marks KC, Banks WR 3rd, Cunningham D, Witman PM, Herman GE. Analysis of two candidate genes for Basan syndrome. *Am J Med Genet A*. 2014;164A(5):1188-1191.

76. Kazakevych J, Denizot J, Liebert A, et al. Smarcad1 mediates microbiota-induced inflammation in mouse and coordinates gene expression in the intestinal epithelium. *Genome Biol*. 2020;21(1):64.

77. Hakem R, de la Pompa JL, Mak TW. Developmental studies of Brca1 and Brca2 knock-out mice. *J Mammary Gland Biol Neoplasia*. 1998;3 (4):431-445.

78. Marot D, Opolon P, Brailly-Tabard S, et al. The tumor suppressor activity induced by adenovirus-mediated BRCA1 overexpression is not restricted to breast cancers. *Gene Ther*. 2006;13(3):235-244.

79. Tian XX, Rai D, Li J, et al. BRCA2 suppresses cell proliferation via stabilizing MAGE-D1. *Cancer Res*. 2005;65(11):4747-4753.

80. Densham RM, Garvin AJ, Stone HR, et al. Human BRCA1-BARD1 ubiquitin ligase activity counteracts chromatin barriers to DNA resection. *Nat Struct Mol Biol*. 2016;23(7):647-655.

81. Doiguchi M, Nakagawa T, Imamura Y, et al. SMARCAD1 is an ATP-dependent stimulator of nucleosomal H2A acetylation via CBP, resulting in transcriptional regulation. *Sci Rep*. 2016;6:20179.

82. Xiao S, Lu J, Sridhar B, et al. SMARCAD1 contributes to the regulation of naive pluripotency by interacting with histone citrullination. *Cell Rep*. 2017;18(13):3117-3128.

83. Kalimuthu SN, Chetty R. Gene of the month: SMARCB1. *J Clin Pathol*. 2016;69(6):484-489.

84. Soininen R, Schoor M, Henseling U, et al. The mouse enhancer trap locus 1 (Etl-1): a novel mammalian gene related to Drosophila and yeast transcriptional regulator genes. *Mech Dev*. 1992;39(1-2):111-123.

85. Nousbeck J, Burger B, Fuchs-Telem D, et al. A mutation in a skin-specific isoform of SMARCAD1 causes autosomal-dominant adermatoglyphia. *Am J Hum Genet*. 2011;89(2):302-307.

86. Klages-Mundt NL, Kumar A, Zhang Y, Kapoor P, Shen X. The nature of Actin-family proteins in chromatin-modifying complexes. *Front Genet*. 2018;9:398.

87. Lans H, Marteijn JA, Vermeulen W. ATP-dependent chromatin remodeling in the DNA-damage response. *Epigenetics Chromatin*. 2012;5:4.

88. O'Donnell PH, Stark AL, Gamazon ER, et al. Identification of novel germline polymorphisms governing capecitabine sensitivity. *Cancer*. 2012;118(16):4063-4073.

89. Hoshijima K, Jurynec MJ, Grunwald DJ. Precise editing of the zebrafish genome made simple and efficient. *Dev Cell*. 2016;36(6): 654-667.

90. Li MY, Zhao LY, Page-McCaw PS, Chen WB. Zebrafish genome engineering using the CRISPR-Cas9 system. *Trends Genet*. 2016;32(12): 815-827.

91. Xiao A, Wang Z, Hu Y, et al. Chromosomal deletions and inversions mediated by TALENs and CRISPR/Cas in zebrafish. *Nucleic Acids Res*. 2013;41:e141.

92. Kim BH, Zhang G. Generating stable knockout zebrafish lines by deleting large chromosomal fragments using multiple gRNAs. *G3 (Bethesda)*. 2020;10(3):1029-1037.

SUPPORTING INFORMATION

Additional supporting information may be found online in the Supporting Information section at the end of this article.